NASDA-TMR-950006T

NASDA Technical Memorandum

A Study of Flight Trajectories to Lunar Orbits via Low Thrust Propulsion and Gravity Capture

October 1996

NASDA

NASDA-TMR-950006T

NASDA Technical Memorandum

A Study of Flight Trajectories to Lunar Orbits via Low Thrust Propulsion and Gravity Capture

Koji Yamawaki

Future Space Systems Laboratory, Systems Engineering Department,
Office of Research and Development

National Space Development Agency of Japan

Contents

A Study of Flight Trajectories to Lunar Orbits via Low Thrust Propulsion and Gravity Capture

by Koji Yamawaki
Future Space Systems Laboratory, Systems Engineering Department, Office of Research and Development, National Space Development Agency of Japan

Introduction

In lunar and planetary exploration missions, the use of an engine with high specific impulse such as electrical propulstion thrusters as the orbital transfer propulsion system is highly desirable in making small exploration spacecraft possible.

Normally, in the case of the electrical propulsion thruster such as an ion engine, the specific impulse of 3,000 seconds or more is obtained, making it possible to greatly reduce the fuel weight ratio of the spacecraft. For example, in the case of the flight from a low earth orbit to a low lunar orbit, the fuel weight ratio is about 80% in a conventional chemical rocket engine, but this decreases to about 20% with electrical propulsion from the ion engine, greatly improving the chances of achieving smaller size in the spacecraft.

However, since the thrust being obtained from ion engines is very small, the orbital transfer from low altitude of several hundred kilometers is naturally very slow, occurring in a spiral orbit of gradually increasing altitude, so that the number of days required for the flight increases greatly. In addition, since rapid acceleration and deceleration for the escape from the low earth orbit and entering the lunar orbit are not available, it is necessary to follow such a flight path as allows gradual transfer from the low earth orbit to the lunar orbit with low thrust. The existence of these kind of gravitational capture orbits has been reported by researchers of NASA, ISAS, etc.[1,2,3)]

Viewed in a coordinate system in which the direction from the earth to the moon is fixed, the aforementioned gravitational capture orbits is near the path through which the spacecraft

can approach to the moon with minimum energy; this path passes near the Lagrange point between the earth and the moon.[4,5]

Additionally, since total energy can be constant unless thrust is used, the spacecraft breaks away from the moon. Therefore, unless velocity relative to the moon is reduced and orbital altitude decreased within a limited time, it is not possible to enter a stable lunar orbit.

This report gives the concepts and conditions for flight path generation that requires only very low thrust acceleration on the order of 10^{-5}G, and examples of numerical calculation of flight paths based on this.

2. Flight path configuration and generation conditions

2.1 Concept and configuration of a low thrust lunar flight path

Basic problems relating to the generation of the flight path to the moon can be considered separately in each part as follows:

(1) Spiral earth orbit in the region in which the earth's gravity is dominant.

(2) Lunar capture orbit in the region in which the earth's gravity and the moon's gravity compete.

(3) Spiral lunar orbit in the region in which the moon's gravity is dominant.

Fig. 1 shows the concept and configuration of the whole flight path, considering the characteristics of orbits generated at low thrust.

First, in the spiral earth orbit, nearly continuous thrusting gives a nearly circular orbit with gradually increasing orbital altitude. In this early phase, since the effect of the J_2 term of the gravitational potential is large, the main task of the phase is to use this effect to change the orbital plane. In later phase, the effect of the J_2 term weakens, and fine adjustment of the orbital plane by thrust vector control becomes necessary. In this phase the eccentricity does

not increase rapidly, and the target orbit is a quasi-circular orbit of radius 150,000km or less. The required inclination of this orbital plane to the moon's orbital plane is mainly determined by the path and the time of the penetration to the lunar orbit. However, since the number of days required for the flight varies with, for example, fluctuations in the thrust, this orbit will not automatically link to the intended lunar capture orbit. Consequently, even after the arrival into the intended orbit, it is necessary to adjust the time and make orbital corrections to obtain the appropriate conditions for the approach to the moon. The reason for choosing a quasi-circular orbit of radius 150,000km or less as this target orbit (referred to below as the parking orbit) is to minimize perturbations due to the moon's gravity.

The lunar capture orbit is a flight path from the parking orbit to the stable orbit around the moon; it consists of a transfer phase in which the eccentricity is increased, a flight phase of approach to the moon by coast flight, and a transfer phase of entry to a stable lunar orbit (hereafter these phases will be referred to the P transfer phase, the coast flight phase and the Q transfer phase, respectively; the end point of the P transfer orbit will be called the P point, and the starting point of the Q transfer orbit, the Q point). Among these, the coast flight path that links the P point and the Q point is a trajectory that reaches the moon supplemented by the gravity, but this trajectory, continuing its coast flight, escapes from the moon afterall. For this reason, it is necessary to reduce the velocity of the spacecraft relative to the moon and transfer to a stable lunar orbit within an appropriate term. However, depending on the position vector and the velocity vector of the Q point (also called the Q point state variables) defined in a coordinate frame with origin at the moon's center, there are cases in which it is not possible to find a Q transfer orbit that transfers to a stable orbit. Whether or not it is possible to obtain a Q transfer orbit that links to a stable lunar orbit is strongly related to the

thrust magnitude that can be used for the orbital transfer and the magnitude of the relative velocity to enter the moon.

The spiral lunar orbit is a phase of lowering of the orbit with nearly continuous thrusting (deceleration); like the spiral earth orbit, it consists of 2 phases. In this spiral orbit, once the eccentricity is suppressed to a small value, it does not increase again even if continuous thrust is applied. Therefore, if the eccentricity increases in this former phase, it is necessary to decrease the eccentricity by unilateral deceleration on the perigee side to prepare for the continuous thrusting in the latter phase. If the eccentricity cannot be decreased in the former phase, the number of flight days will be increased because the period of time for decelerating is limited to the perigee side.

2.2 Properties and generation of the spiral orbit

In a quasi-circular orbit of small eccentricity e, if we let S and T be small directions in the direction of the orbital radius and in the direction that is parallel to the orbital plane and perpendicular to the orbital radius, respectively, the rate of change of the semi-major axis of the orbit da/dt becomes approximately[4]:

$$da/dt=2(a^3/\mu)^{1/2}(Se\sin f+T) \quad (1)$$

Here f is the true anomaly, and μ is the gravitational coefficient in the central force field (hereafter, we will use μ_e ($=3.986\times10^5 km^3sec^{-2}$) for the earth orbit and μ_m ($=4.903\times10^3 km^3sec^{-2}$) for the lunar orbit.

According to Eq. (1), S contributes almost nothing to increasing the orbital radius. Consequently, here we assume that the thrust vector is in the same direction as the velocity vector. In this case, as shown in Appendix A, the eccentricity e is given by:

$e=2(F/m)/(\mu/a^2)$ (2)

so that the eccentricity of the spiral orbit is determined by the thrust acceleration F/m and the gravitational acceleration μ/a^2. Consequently, in the case of low thrust on the order of $F/m = 2\text{x}10^{-4}\text{m/s}^2$, the eccentricity does not exceed 0.05 as far as the earth orbit of radius is 150,000km or less and the lunar orbit of radius is 20,000km or less.

The condition for the entry to a lunar capture orbit from a parking orbit is found by the adjustment of the departure condition at the parking orbit and of the Q point state variable. This problem will not be discussed here, but it is the important problem for future consideration as the Q point targeting problem.

2.3 Properties and generation of the lunar capture orbit

The Q point is the condition that characterizes the lunar capture orbit; it is defined by the position vector and the velocity vector with respect to the moon. Whether or not it is possible to generate the lunar capture orbit for this Q point depends on whether or not the P point in the region where the earth's gravity is dominant can be found by reverse integration from the Q point and on whether or not the Q transfer orbit that links to the spiral lowering orbit with low thrusting can be generated. A Q point for which this kind of P transfer orbit and Q transfer orbit can be generated is a usable Q point.

First, search for a Q point that is linked to the P point by reverse integration. This is a set of state variables consisting of the Q point position vector r_Q and the Q point velocity vector v_Q. Then, a usable Q point must have values that generate an orbit that is a no-thrust orbit with the relative velocity suitable for approaching the moon, and more or less orbits the moon although not permanently stable. If it is a stable lunar orbit, there will not be a coast flight path that connects to the P point, so the Q point is not a usable Q point.

Referring to Fig. 2, in the fixed Earth-Moon coordinate frame in which the x-axis joins the Earth and the Moon and rotates around the z-axis with angular velocity w with respect to inertial space, the so-called pseudo-energy E of a unit mass is expressed in terms of the position vector r and the velocity vector v by the following equation[4]:

$$E=v^2/2-(w\times r)^2/2-\mu_e/r_e-\mu_m/r_m \tag{3}$$

Here r_e and r_m are the absolute values of r_e and r_m, respectively. This relation is obtained by transforming the Jacobian integral of the constrained 3-body problem[5] into the relation in units of energy. If we take the absolute value r_{em} of the vector r_{em} from the earth to the moon and the absolute value w of the angular velocity w in the E-M coordinate system to be fixed, the pseudo-energy E_0 when v is zero is related to the Jacobian integration constant C by the relation:

$$E_0=-(r_{em}w)^2\times(C/2) \tag{4}$$

Also, from Eq. (3), the pseudo-energy of a Q point that is 45,000km above the lunar north pole and has a velocity of 350m/s in the x direction (the velocity corresponding to an eccentricity of 0.12 obtained from the 2-body problem with the moon) becomes -1.588km^2/s^2; this does not change even after the escape from the moon. Fig. 3 shows the pseudo-energy on the straight line joining the earth and the moon (called the L line); the above energy is an energy for which it is possible to escape from the moon with the relative velocity exceeding 300m/s at the Lagrange point (the L point).

Next, if we rewrite Eq. (3) in terms of the semi-major axis a and eccentricity e of the earth orbit, the inclination i_v with respect to the lunar orbital plane and the angle (θ) between the L line and r_e, we obtain approximately:

$$E=-\mu_e/2a-w[\mu_e a(1-e^2)]^{1/2}\cos i_v-\mu_m/r_m+r_e\mu_m\cos\theta/r_{em}^2 \tag{5}$$

so that an approximate relation with the final orbital elements of P transfer is obtained. For reference, if we take E=−1.588km^2/s^2, i_v=15 degrees, and assume that the spacecraft is at a right angle to the L line and 450,000km from the moon, the semi-major axis for an eccentricity of 0.3 is obtained from Eq. (3) to be about 250,000km, so the perigee radius becomes 175,000km and the apogee radius 325,000km. Consequently, the final apogee point of the P transfer orbit almost reaches the L point.

2.4 The region in which the Q point radius exists

The constraints on the Q point radius are found from the magnitude of the thrust and the effect of the earth's gravity. Let us take the Q point to be the perigee of an orbit of eccentricity e_0, with the moon providing the central force field, neglecting the earth's gravity. Then we seek the velocity increment δV necessary to stabilize the orbit. First, starting from the orbit of perigee radius r_0, if the perigee radius r_1 of the orbit generated by the deceleration within half a period is smaller than r_0, then it is possible to obtain stable spiral descent without increasing the eccentricity by switching the thrust ON and OFF roughly every half period. Then, as a condition for stabilizing the transfer orbit, if we assume that the relation:

$$r_1<\kappa r_0 \quad (0<\kappa<1) \tag{6}$$

applies between the perigee radius r_0 of the orbit after stabilization and r_1, then the velocity increment δV must satisfy:

$$\delta V>(\mu_m/r_0)^{1/2}[(1+e_0)^{1/2}-\{2\kappa/(1+\kappa)\}^{1/2}] \tag{7}$$

Here, if we take r_0=45,000km, e_0=0.1 and k=0.8, then δV >35m/s. Consequently, in the case of a spacecraft for which F/m=2x10^{-4}m/s^2, if the deceleration is supposed to be done continuously for about 2 days, then we obtain a rough condition for the entry to the more

stable orbit. In addition, if we let λ be the ratio of the time during which deceleration is possible in the vicinity of the Q point to the orbital period, we obtain:

$$r_0>[\mu_m(1-e_0)^{3/2}[(1+e_0)^{1/2}-\{2\kappa/(1+\kappa)\}^{1/2}(2\pi\lambda F/m)]^{1/2}$$

$$\fallingdotseq 19{,}000/\lambda^{1/2}\text{km} \tag{8}$$

Consequently, if we assume that it is possible to apply decelerating thrust through a half period so that the spacecraft is decelerated only on the perigee side in order to decrease the eccentricity, then, since $\lambda=1/2$, we obtain $r_0>27{,}000$km. Thus, the lower limit of the Q point radius r_0 is determined by the magnitude of the thrust acceleration on the spacecraft. Next, in the case in which the Q point radius is large, the effect of the earth's gravity becomes relatively large, so that the lunar orbit becomes unstable. First, we find the acceleration vector α applied to the spacecraft with respect to an inertial coordinate frame with origin at the moon's center:

$$\alpha=-(\mu_e/r_e^3)\boldsymbol{r}_e-(\mu_m/r_m^3)\boldsymbol{r}_m-\boldsymbol{w}\times(\boldsymbol{w}\times\boldsymbol{r}) \tag{9}$$

Thus, if we assume that the moon moves in a circular orbit around the center of gravity of the earth-moon system, then Eq. (9) can be rewritten as follows:

$$\alpha=(\mu_m/r_m^2)\boldsymbol{i}_m-(2\mu_e r_m\cos\phi/r_{em}^3)\boldsymbol{i}_e-(r_m w^2\cos\psi)\boldsymbol{i}_n \tag{10}$$

where $\boldsymbol{i}_m$ and $\boldsymbol{i}_e$ are the unit vectors from the spacecraft to the moon and the earth, respectively, ϕ is the angle between the direction from the earth to the moon and $\boldsymbol{i}_m$, ψ is the angle between the angular velocity of revolution of the moon w and r_m, and $\boldsymbol{i}_n$ is the unit vector of the vector of w. However, since the terms other than the 1st term on the right side of Eq. (10) tend to disrupt the stable elliptical movement of the spacecraft, they must be made suitably small compared to the 1st term. Then, if, as a necessary condition for the orbit

being stable, we require that the sum of the 2nd term and the 3rd term be smaller than the 1st term:

$$(2\mu_e r_m/r_{em}^3+r_m w^2)<\mu_m/r_m^2 \tag{11}$$

then we obtain the following relation:

$$r_m<r_{em}\{\mu_m/(2\mu_e+w^2 r_{em}^3)\}^{1/3}\fallingdotseq 61{,}000\text{km} \tag{12}$$

From the above analysis, usable Q points for the spacecraft with thrust acceleration $2\text{x}10^{-4}\text{m/s}^2$ can be said to have a possibility of existence in the region of orbital radius from 30,000 to 60,000km.

2.5 Constraints on the Q point

The problem to find the flight path which approaches the lunar orbit using a low thrust, rendezvous with the moon for an appropriate period and approaches the moon softly is not other than the 3-body problem; the region in which the Q point exists can be expected to depend strongly on not only the magnitudes of the Q point position vector r_Q and the Q point velocity vector v_Q, but also on their directions. This problem is also related to the inclination angle of the penetration orbit; it is necessary to treat at least the ring-shaped region shown in Fig. 4 (this is called the Q ring) as a region in which the Q point can exist. Is there not any additional region beyond the Q ring shown in Fig. 4 where a usable Q point can exist? In the following discussion, referring to an example of numerical calculation of a lunar capture orbit expressed in the E-M coordinate frame in the case in which r_{em} is fixed, we search for the specific region of Q point existence and determine the constraints on the usable Q point.

Fig. 5 shows a 3-dimensional flight path (the dots are at intervals of 1 day) for a Q point radius of 45,000km; the approach is from below the moon's orbital plane and the path passes

through the Q point above the North Pole. Fig. 6 and Fig. 7 show flight paths for a Q point radius of 40,000km, with the Q point on the moon's orbital plane. In both cases the velocity at the Q point reaches 350m/s; escape from the moon occurs not later than 10 days after passing through the Q point. Since these flight paths are sets of Q points in a broad sense, we can assume that there exist many Q points surrounding the moon. Conversely, since one of the Q points is representing many Q points, candidates for usable Q points are constrained to lie on the ring in Fig. 4. In Fig. 7 we have chosen a Q point, r_Q, which is parallel to the line joining the earth and the moon (the L line) and which exists on the circular orbit going around the moon. But, this is a special path in which the Q point is reached about 8 days after passing the vicinity of the L point and swinging around the moon. This is a very interesting orbit to which approach occurs at low inclination angle, but here we believe that it is better not to treat this point as a standard Q point.

In Fig. 4, the angle ϕ_Q between r_Q and the moon's north polar axis (the complement of the latitude, called the Q angle) is a parameter that determines the orbital inclination angle. As shown in Fig. 6, seen from the earth the usable Q point exists in the right side of the Q ring; in the left side it is difficult to find Q point conditions such that the flight path escapes from the moon and links to the P transfer orbit. In the example shown in Fig. 8, the Q angle is -90 degrees to the left; the path shown is obtained by reverse integration in the case in which the Q point radius and the Q point velocity are the same as in Fig. 6 and only the Q point velocity increases to an eccentricity of 0.99(eccentricity). With these Q point conditions the escape from the moon is not possible; even if the escape were possible, it would not be possible to obtain a flight path that approaches the earth. Consequently, there is no Q point that links with the P point. This is an interesting problem related to the energy in the E-M coordinate system, but analytical discussion is omitted here. From the above discussion, to

generate a low thrust orbit it is sufficient for the usable Q point to satisfy the following conditions.

(1) The penetration direction of the spacecraft is approximately along the L line toward the earth. Approach from the opposite direction is inconceivable.

(2) The lunar escape flight path from the Q point to the P point is a no-thrust orbit with perigee radius of 200,000km or less.

(3) Taking the Q point radius to be 45,000 ± 10,000km and the Q angle to be 0 to 180 degrees, the Q point velocity vector is orthogonal to the Q point position vector.

(4) The lunar orbit is stabilized, normally by decelerating on the perigee side, from the time of passage through the Q point.

(5) With a semi-major axis of the Q transfer orbit of 20,000km, the eccentricity becomes 0.2 or less.

2.6 Example of calculation of the region in which Q points for which lunar capture is possible exist

Fig. 9 shows the lower limit of velocity for which the escape from the moon is possible in a coast flight as found by reverse integration from the Q point above the north pole, and the upper limit of velocity reaching a stable lunar orbit of eccentricity 0.2 or less within several orbits of the powered flight. The lower limit fluctuates on the order of 20m/s depending on the time of arrival at the moon because of the moon's elliptical motion; the graph in the figure shows its maximum values. At a Q point radius of 55,000km or more, the orbit becomes somewhat unstable, so the range of condition computation was taken to be 45,000 ± 10,000km. In addition, the deceleration control in the Q transfer phase is according to the eccentricity control method discussed in section 3; normally, it starts 2 to 3

days before passage through the Q point. The region in which usable Q points can exist is the range of the above Q point radius; it is the region bounded by the limit of possible escape from the moon's gravity and the limit of lunar orbiting stability.

Fig. 10 shows the region within which Q points for which lunar capture is possible can exist in the case in which a lunar orbit that is parallel to the moon's path is generated. In this example, the Q point was set in the direction 90 degrees from the L point, but compared with Fig. 9, the region within which Q points can exist is much smaller than that in the case of a large orbital radius. The reason for this is that, as can be seen from the relation between the eccentricity computed from the 2-body problem shown by the dotted line shown in the figure and the Q point velocity, although the Q point exists on the apogee side, the logic of decelerating only on the perigee side is applied unconditionally. If, for example, deceleration is applied continuously from 4 days before passage through the Q point until the apogee radius drops to 30,000km or less, and then deceleration control is subsequently applied to decrease the eccentricity, the range of lunar orbiting stability expands as shown by the dashed line in the figure. This kind of continuous deceleration in the Q transfer phase is effective in expanding the region within which Q points exist, but since the perigee point is lowered by deceleration on the apogee side, a problem arises in subsequent eccentricity control. Consequently, it is necessary to monitor the perigee radius and judge whether or not to perform the continuous thrusting.

3. Low Thrust Orbit Transfer

3.1 Spiral ascending orbit transfer

When the direction of the spacecraft thrust vector is aligned with the direction of the velocity vector, and in addition the eccentricity is held at nearly zero and the orbital radius is changed very gradually from r_s to r along a spiral path, the relation between the cumulative value V_T obtained by summing up the velocity increments and the orbital radius is found as an approximate solution to Lagrange's Planetary Equations for the orbital radius or as the limiting solution of a multi-stage very small Hohmann orbital transfer:

$$V_T=(\mu/r_s)^{1/2}-(\mu/r)^{1/2} \tag{13}$$

This V_T, as shown in Appendix B, is the upper limit of velocity increment in the multi-stage Hohmann orbital transfer. If we let F be the thrust, I_{sp} the specific impulse, m_s the initial mass and m the residual mass, the cumulative value V_T of the velocity increment can be written as:

$$V_T=gIsp\log(m_s/m) \quad (g=9.8\mathrm{m/s^2}) \tag{14}$$

Consequently, substituting V_T found from Eq. (13) into Eq. (14), the residual mass ratio m/m_s becomes:

$$m/m_s=\exp(-V_T/gIsp) \tag{15}$$

and the number of flight days t becomes:

$$t=\{gIsp/(F/m_s)\}\{1-\exp(-V_T/gIsp)\} \tag{16}$$

Thus, in a low thrust spiral orbital transfer, if the thrust acceleration F/m_s at the time of the initial mass and the specific impulse Isp are known, the residual mass ratio and the number of flight days are uniquely determined.

Fig. 11 shows the relation between the orbital velocity and the number of flight days with r_s=7,378km and the initial thrust acceleration having the standard value of $2\times10^{-4}\mathrm{m/s^2}$. This gives a flight time of about 10 months until an orbital radius of 150,000km is reached. The

graphs in the cases in which F/m_s fluctuates $\pm 20\%$ from the standard value are also shown; if orbital control is applied based on these 3 thrust levels, the orbital height and the number of flight days can be easily adjusted.

3.2 Orbital plane transfer

The inclination angle of the orbital plane with respect to the lunar orbital plane is an important parameter which plays a significant role in determining the approach orbit to the moon; the shift of the ascending node of the spacecraft orbital plane due to the oblateness of the earth is used in this adjustment. That is to say, even in the case in which the spacecraft is in no-thrust flight in a circular orbit of radius r, the right ascension Ω of the ascending node changes because of perturbation forces due to the J_2 term of the gravitational potential. The relation of this to elapsed time becomes[4)]

$$\Omega=\Omega_0-(3/2)(\mu^{1/2}J_2R_e^2\cos i/r^{7/2})t \tag{17}$$

where Ω_0 is the right ascension of the ascending node at $t=0$, R_e is the earth's radius and i is the inclination angle of the orbital plane with respect to the equatorial plane. Further, substituting into Eq. (13) and Eq. (16) and applying the calculus of variations, we obtain the relation for the fuel consumption rate $\nu=F/gIsp$:

$$(2ugIsp/m)\delta t=(\mu/r^3)^{1/2}\delta r \tag{18}$$

Consequently, the variational form of equation (17) can be rewritten as:

$$\delta\Omega=-\frac{3\mu m_s\exp[-V_T/gIsp]J_2R_e^2\cos i}{4r^5 v\ gIsp}\delta r \tag{19}$$

which gives us a relation between the variation δr of the orbital radius r and the variations $\delta\Omega$ of the right ascension Ω of the ascending node. If we numerically integrate Eq. (19), we

can find the right ascension Ω of the ascending node with respect to the orbital altitude, which converges to a specific value at orbital altitude of 20,000km and higher.

Next, we seek a relation between the right ascension of the ascending node of the spacecraft's orbital plane and the inclination angle of the orbital plane with respect to the plane of the moon's path. Let i_e be the inclination angle of the ecliptic with respect to the equator, Ψ the difference of longitude between the ecliptic longitude of the ascending node of the equator and the ecliptic longitude of the ascending node of the moon's path, and i_m the inclination angle of the moon's path with respect to the ecliptic. Then, if Ω is known, the unit vector n_0 in the direction normal to the spacecraft's orbital plane in the coordinate frame fixed in the earth is transformed to the unit vector n in the coordinate frame fixed in the plane of the moon's path by the following equation, using the Quaternion (also called Euler's parameter) which expresses rotation through the above angles:

$$n=\rho_4^*\rho_3^*\rho_2^*\rho_1^*n_0\rho_1\rho_2\rho_3\rho_4 \tag{20}$$

Here ρ_i and n_0 can be expressed by the following equations, considering rotation in their respective coordinate frame:

$$\rho_1=\cos(\Omega/2)+e_3\sin(\Omega/2) \tag{21}$$

$$\rho_2=\cos(i_e/2)+e_1\sin(i_e/2) \tag{22}$$

$$\rho_3=\cos(\Psi/2)+e_3\sin(\Psi/2) \tag{23}$$

$$\rho_4=\cos(i_m/2)+e_1\sin(i_m/2) \tag{24}$$

$$n_0=-e_2\sin i+e_3\cos i \tag{25}$$

where e_1, e_2 and e_3 are parameters which can be calculated as follows:

$$e_1^2=e_2^2=e_3^2=-1 \tag{26}$$

$$e_1 e_2 = -e_2 e_1 = e_3 \tag{27}$$

$$e_3 e_3 = -e_3 e_2 = e_1 \tag{28}$$

$$e_3 e_1 = -e_1 e_3 = e_2 \tag{29}$$

ρ_i^x is in a conjugate relation with ρ_i, and defined as follows:

$$\rho_1^* = \cos(\Omega/2) - e_3 \sin(\Omega/2) \tag{30}$$

From Eq. (26) to (29), we have the more general relation:

$$\rho_i^* \rho_i = 1 \quad (i=1,2,3,4) \tag{31}$$

Here, noticing that the ascending node of the equator and the ascending node of the moon's path are at nearly the same ecliptic longitude, the inclination angle i_v of the spacecraft's orbital plane with respect to the plane of the moon's path fluctuates within the approximate limits:

$$|i-(i_e-i_m)| \leqq i_v \leqq |i+(i_e-i_m)| \tag{32}$$

due to fluctuations of the right ascension Ω of the ascending node. Consequently, since i_e=23.5 degrees and i_m=5.1 degrees, by adjusting Ω the inclination angle i_v can be adjusted within the limits $i \pm$ 18.4 degrees.

Fig. 12 shows the relation between the orbital radius and i_v computed from Eq. (20) for i=30 degrees, Ω_0=330 degrees. In this case, by adjusting the thrust $\pm$ 20%, the inclination angle i_v until an altitude of 20,000km is reached can be adjusted within the limits of 12 to 39 degrees. i_v is one of the conditions of a parking orbit for the purpose of entering an orbit around the moon that has a specified inclination angle, and is determined by reverse integration from the Q point.

3.3 Increase of the eccentricity in the P transfer orbit

According to Eq. (2), the eccentricity of the spiral orbit for reaching the L point from the parking orbit by continuous low thrust of 2×10^{-4}m/s^2 is 0.09 degree; and the semi-major axis of the orbit becomes about 300,000km. Substituting this condition into Eq. (5) the orbital energy E is found to be -1.566km^2/s^2, and the velocity of penetration to the moon is increased 60m/s over the 350m/s found in section 2.3. Thus, in the spiral orbit generated by continuous thrust the deceleration condition in the Q transfer phase becomes more severe, so it is desirable to perform orbital transfer in the P transfer phase by applying thrust for half an orbit to increase the eccentricity. To obtain simple regularity of orbital control, hereafter we will use:

thrust ON when $r<a$

thrust OFF when $r \geqq a$ (33)

as the thrust ON/OFF control condition.

In addition, even in the case of departure from the same Q point, if the thrust ON/OFF condition changes, then the parking orbit elements obtained by reverse integration will also change. Consequently, if in place of a uniform condition such as that of Eq. (33) we use the true anomaly f (-180 degrees to +180 degrees):

thrust ON when $|f_1|<f_0$

thrust OFF when $|f_1| \geqq f_0$ (34)

and treat f_0 as an object of control, then the boundary conditions between the parking orbit and the P transfer orbit can be adjusted. Here we do not generate an orbit using Eq. (34).

3.4 Stabilization and decrease of the eccentricity in the Q transfer orbit

As shown in Fig. 5 through 7 of the previous section, a spacecraft that approach the moon in coast flight does not enter a stable orbit, but returns to the region in which the earth's gravity predominates. Therefore, in contrast to the previous section, it is necessary to apply the deceleration on the perigee side for several days before and after passage through the Q point to decrease the spacecraft's energy.

Fig. 13 shows the process of stabilization of the lunar orbit during 12 days after passage through the Q point for 4 cases (Q-3 to Q-1 and Q0) in which the spacecraft is decelerated from a few days before passage through the Q point. For example, in case of Q-3, the deceleration is done 3 days before passage through the Q point. In the cases except for Q0 the spacecraft does not pass through the Q point anymore, but by applying the deceleration before passage through the Q point the Q transfer orbit is rapidly stabilized, and even as this is done, the orbital inclination angle does not deviate greatly.

3.5 Spiral descending transfer

Reverse thrusting is applied continuously to decelerate the spacecraft and decrease the eccentricity while retaining a circular orbit. Normally, in the low thrust spiral descending orbit transfer, the increase of the eccentricity tends to be suppressed. However, in a case in which the eccentricity is not decreased by the effect of the earth's gravity and orbital control, it is necessary to apply the deceleration only on the perigee side until the specified eccentricity is reached, as in the case of orbital control in the Q transfer phase. The residual mass ratio and the number of days required can be found from the relations in section 3.1.

4. Examples of numerical calculation of lunar capture orbit

4.1 Polar entry flight path

First, a flight path in which the Q point is above the North Pole is generated. Since the result obtained for the spiral orbit is as discussed in section 2.2, it is omitted here. We now compute the flight path for arriving at a parking orbit by F/m=0.0233mG. In addition, the lunar capture orbit fluctuates somewhat depending on the date to intersect the moon (the number of days from the moon's passage through the perigee to the spacecraft's passage through the Q point); here we take this to be 0 days.

Fig. 14 shows the lunar capture orbit for Q point radius 45,000km, Q point penetration velocity 350m/s (eccentricity 0.122) and polar entry. The initial conditions of the P transfer orbit are found by reverse integration from the Q point. Thrusting is ON in the parts of orbits shown by thick lines. Orbital Parameters are in the figure, the upper row gives the vector normal to the orbital plane and the lower row gives, from left, the semi-major axis, the eccentricity and the period (in hours). In the P transfer phase, by applying unilateral thrust in accordance with Eq. (33) for 4 orbits a parking orbit of radius about 150,000km is linked to the Q point; the orbital inclination angle i_v is about 15 degrees and the number of flight days in this phase is about 42. In the generation of the Q transfer orbit, forward integration is done starting 4 days before passage through the Q point; Eq. (33) are applied as the deceleration control condition.

Fig. 15 shows the coast flight path from the P point in Fig. 14 and the Q transfer orbit which are coordinatized in the inertial frame perpendicular to the plane of the moon's path centered at the moon. The path reaches an approximately circular orbit (eccentricity about 0.02) of the radius of 20,000km or less about 2 weeks after passage through the Q point, and which becomes nearly the polar orbit, which goes round the moon.

4.2 Equatorial entry flight path

Fig. 16 shows a lunar capture orbit with equatorial penetration at Q point radius 45,000km and Q point penetration velocity 290m/s (eccentricity 0.23, apogee side), r_Q of which lies on the plane of the moon's path in a direction perpendicular to the L line. The inclination angle of the orbit that is generated becomes 0 degrees. This Q point lies on the boundary region of the lower limiting values in Fig. 10; a parking orbit of radius 115,000km and eccentricity 0.05 is reached in about 60 days. In the numerical calculation when the penetration velocity increases, the perigee radius of the P transfer orbit decreases and the number of flight days taking to reach the parking orbit increases. Fig. 17 shows two cases of lunar capture orbits, with and without deceleration, which are coordinatized in the inertial frame centered at the moon. By applying deceleration control from 4 days before passage through the Q point, the path reaches a quasi-circular orbit of radius about 20,000km 10 days later.

5. Orbital control

5.1 Orbital control in the P transfer phase

The nominal flight path in the P transfer phase is generated by the ON/OFF sequence control of the thrust. However, in the orbital control in which only a predetermined ON/OFF time sequence is applied, the spacecraft will have a possibility not to approach the moon by thrust fluctuations and the solar pressure will make it impossible to approach to the moon.

Fig. 18 shows the P transfer orbits with and without the thrust errors of $\pm$ 1% and generated under the same conditions as used in Fig. 14 except the thrust errors. Since the

orbit deviates considerably with even a 1% thrust error (corresponding to 2×10^{-2}G), it is conceivable that even the effect of solar pressure could make it impossible to reach the Q point. Consequently, in the flight requiring many days, it is necessary to apply the orbital control in response to fluctuations at least in the coast flight phase.

In a case in which external disturbances due to solar pressure or thrust errors are large, it will become impossible to correct the orbit errors accumulated in the coast flight phase by applying the orbital control. In this case, the orbital control during the powered flight is important; the control method described below (simply called the thrust control method) is used. First, orbital errors related to the motion in the central force field and orbital errors in the direction perpendicular to the orbital plane are corrected by changing the thrust vector direction $\pm$ 8.5 degrees (0.15 radian) from the nominal direction. Regarding the former, the equation of motion of radius r is as follows:

$$d^2r/dt^2=v_t^2/r-\mu_e/r^2 \tag{35}$$

then we find:

$$\delta s_r=\delta_r+2rv_t\delta v_t/(2\mu_e/r-v_t^2) \tag{36}$$

where v_t is the velocity in the orbital plane perpendicular to the radial direction. With regard to the latter, the distance error δr_n and the velocity error δv_n in the direction perpendicular to the orbital plane are added to give:

$$\delta s_n=\delta r_n+\kappa_0\delta v_n \tag{37}$$

Then 3-value control of the thrust direction is applied to δs_r and δs_n. The reason for applying this kind of constraints to the angle of change is to prevent the reduction loss of thrust in the nominal direction. In addition, adding errors of position and velocity in the orbital plane in the direction perpendicular to the radial direction we find:

$$\delta s_t = \delta r_t + \kappa_1 \delta v_t \tag{38}$$

and 3-value control(±30%) is applied to the average thrust. Fig. 19 shows the effect of applying the above thrust control method. The top set of numbers in the figure gives orbital errors in the case in which the perturbation guidance discussed in the next section is applied in response to a 10% thrust error from 10 days before; the other sets of numbers are with no guidance and thrust errors of +10% and -10%. Within each set the upper row gives errors of position(km) and the lower row gives errors of velocity(m/s). According to this, if thrust control is applied in the P transfer phase, the spacecraft can be accurately guided to the Q point by the perturbation guidance in the coast flight phase. In addition, if the orbit is corrected during no-thrust flight in the P transfer phase, the cumulative orbital errors due to solar pressure etc., can be decreased every orbit, increasing the accuracy of guidance to the Q point.

5.2 Orbital control in the coast flight phase

The orbital correction in this phase is done by perturbation guidance. First, the position error δr and δv and velocity error vectors are added to give:

$$\delta s = \delta r + \kappa_2 \delta v \tag{39}$$

and the thrust vector is adjusted in the δs direction. Regarding the component of Eq. (39) in the radial direction, a correction is applied for the effect of motion in a central force field according to Eq. (36). In the above control, a zone of insensitivity is established corresponding to position error of ± 200km and velocity error of ± 2m/s. Discussion of this point is omitted here.

Fig. 20 shows the flight paths with and without guidance in the case in which the position and velocity errors at -10 days (roughly at the P point) are 5,000km and 20m/s respectively for each axis in the 3-dimensional E-M frame. In the case of no guidance, on the day of planned penetration to the moon, the position error radius becomes about 35,000km and the velocity error radius 227m/s, and the moon is not reached anymore. However, if perturbation guidance is applied during a coast flight, the Q point is reached with position error radius of not more than 200km and velocity error radius of not more than 2m/s. Thus, since orbital control in the inertial coast phase is indispensable in a lunar capture orbit, it is desirable for the flight time between the P point and the Q point to be 10 days or more. An example of the error sensitivity coefficient matrix between the P point and the Q point is given in Appendix C.

5.3 Orbital control in the Q transfer phase

Fig. 21 shows Q transfer orbits until the 12th day for 3 types of Q point above the moon's north pole. If the Q point radius and the eccentricity are adjusted, in all 3 cases deceleration control starts from about 3 days before arrival at the Q point and similar Q transfer orbits are followed.

Fig. 22 shows Q transfer orbits for velocity errors in the orbital plane of $\pm$ 10m/sec 4 days before passage through the Q point. The transfer orbits are stable, and the eccentricities after 12 days are all 0.1 or less. Error of direction perpendicular to the orbital plane is the principal cause of inclination angle error, but is not an obstacle to stabilization of the orbit.

6. Conclusions

In this report, we have generated flight paths through which a spacecraft can approach from a low earth orbit to a low lunar orbit with low thrust propulsion on the order of 0.02mG. We have also discussed basic orbital control problems centered on lunar capture orbits. In addition, considering the characteristics of low thrust propulsion, the total path has been broadly divided into 3 flight phases. Based on this classification, the orbital control problems, number of flight days and amounts of fuel consumed are presented for each phase of a nominal polar entry flight path in Table 1.

However, it is difficult to analytically express the conditions for orbital transfer from a parking orbit to the lunar approach point. In addition, since the moon is in elliptical motion, the lunar capture orbit derived from the Q point varies depending on the day on which the moon's path is intersected; therefore it is not clear whether or not there exists a direct guidance method for this phase. Therefore, at present it is necessary to repeatedly perform reverse integration from the Q point in order to generate orbits, and find the nominal flight path from the parking orbit that matches the timing and the orbital transfer conditions for that purpose by trial and error.

Although the above problem is not yet solved, in this report we have generated specific flight paths, and discussed the overall flight plan and the basic problems of orbital control in each phase. In particular, the conditions for establishing the Q point have been determined not only by orbital simulation but, in part, analytically. In addition, we have obtained a prospect that by applying simple orbital control in the P transfer and the Q transfer phases and orbital correction in the lunar capture orbit, we can guarantee the entry to stable lunar orbits with the thrust conditions in this report. Finally, only very small thrusts can be obtained with electrical propulsion such as an ion engine, and the time for flights to the moon by this

thrust becomes very long. This is generally not desirable from the point of view of the design of equipment to be carried on the spacecraft, its operation and monitoring control. In addition, even if the effect of gravitational supplementation is taken into account, spiral orbital transfer cannot be said to be more efficient than Hohmann orbital transfer from the point of view of the velocity increment that is needed. In order to decrease the flight time to 1 to 2 months, solve the above problems in the orbital transfer and make it possible to design a more efficient spacecraft, it is necessary to have the specific impulse of 1,000 seconds or more on the order of 1 to 2N thrust. Consequently, if in the future it is going to be necessary to construct an economical system for transporting supplies between the earth and the moon, and to have a spacecraft that shuttles between the earth orbit and the lunar orbit, then it is necessary to develop a high specific thrust propulsion system as mentioned above, and to conduct active research on orbital transfer and guidance control corresponding to the magnitude of the thrust obtained.

References

1) Delbruno, E.A., *Lunar Capture Orbits, A Method of Constructing Earth-Moon Trajectories and the Lunar Gas Mission*, AIAA-87-1054, Colorado Springs, Colorado, 1987.

2) Korsmeyer, D.J., *A Cislunar Guidance Methodology and Model for Low Thrust Trajectory Generation*, AAS 91-433, Proceedings of the AAS/AIAA *Astrodynamics* Conference, Durango, Colorado, Aug. 1991.

3) H. Yamakawa, J. Kawaguchi, et al, "On Earth-Moon Transfer Trajectory with Gravitational Capture," AAS-93-633 AAS/AIAA Astrodynamics Specialist Conference, Victoria, Canada, Aug. 1993.

4) Roy, A.E., *The Foundations of Astrodynamics*, The Macmillan Company, London, 1965.

5) Araki, Toshima, *Astronomical Dynamics*, Koseisha, 1980.

<<Appendix A: Properties of the Eccentricity in a Low Thrust Propulsion Spiral Orbit>>

An approximate relation between the orbital radius and eccentricity can be easily found from the quasi-spiral orbit generated by very small impulsive velocity increments at half-orbit intervals, at perigee and apogee.

First, in the case in which the initial orbit is a circle of radius a, the eccentricity produced by the initial velocity increment δV is approximately:

$$e=2\delta V\times(a/\mu)^{1/2} \quad \text{(A-1)}$$

and the orbit returns to a circle at the next apogee thrusting. Then, using the period $T(=2\pi(a^3/\mu)^{1/2})$ and the propulsion acceleration F/m, the impulsive velocity increment δV per a semi-circular arc in the tangential direction at perigee and apogee becomes:

$$\delta V=(F/m)\times T\times(1/2)\times(2/\pi)$$

$$=2(F/m)\times(a^3/\mu)^{1/2} \quad \text{(A-2)}$$

Substituting Eq. (A-2) into Eq. (A-1) and averaging the eccentricities at perigee and apogee gives:

$$e=2(F/m)/(\mu/a^2) \quad \text{(A-3)}$$

To confirm that the above equations are correct, we assume that $F/m=2.3\times10^{-4}\text{m/s}^2$ and a=115,000km, and find the eccentricity from Eq. (A-3) to be e=0.015. In numerical calculations the eccentricity fluctuated between 0 and 0.025; the time average agreed well with the analytical solution. As an example of a case in which the increase of eccentricity for a thrust acceleration on the order of 2.3×10^{-4}m/s is small, we use Eq. (A-3) and find the eccentricity in a parking orbit of radius 150,000km to be e=0.026; even at the time of arrival at the Lagrange point it is e=0.10. This also agrees well with the result of numerical calculation. An effective way to increase the eccentricity is thrust for half an orbit on the

perigee side. First, from Eq. (A-3), after departure from a circular orbit of radius r_0 the eccentricity e_0 after the first half-orbit propulsion becomes:

$$e_0(1-e_0)^2=4(F/m)/(\mu/r_0^2) \tag{A-4}$$

The eccentricity e_N after the subsequent Nth half-orbital thrust is given approximately by the following equations:

$$e_N=\sum_{i=0}^{N} e_i, \quad e_i=e_0(1+\sum_{j=0}^{j=1} e_j)^2 \tag{A-5}$$

For reference, we numerically calculate the spiral orbit produced by approximately half-orbital propulsion from a circular orbit of radius 150,000km. After 4 orbits we obtain an elliptical orbit of perigee radius about 180,000km, apogee radius about 340,000km and eccentricity about 0.3. Meanwhile, in Eq. (A-4), e_0 becomes 0.059. Consequently, from Eq. (A-5), the eccentricity after another 3 orbits with half-arc propulsions becomes 0.285, in approximate agreement with the numerical solution.

<<Appendix B: Continuous Low-Thrust Orbital Transfer and Hohmann Orbital Transfer>>

In orbital transfer with continuous low-thrust propulsion, the cumulative value of velocity increment is found from the initial and final values of the orbital radius. Consequently, since the cumulative velocity increment is independent of how the flight path is partitioned into segments, if we take $r_s=r_0$ and $r_f=r_n$ then we obtain the relations:

$$V_T=\sum_{i=1}^{n}\delta V_i \tag{B-1}$$

$$\delta V_i=(\mu/r_{i-1})^{1/2}-(\mu/r_i) \tag{B-2}$$

Meanwhile, in a multi-stage Hohmann orbital transfer, if we consider only the case in which the orbital radius increases monotonically, regardless of whether a circular orbit is entered in an intermediate stage before return to an elliptical orbit or the spacecraft moves directly from one elliptical orbit to another, the cumulative velocity increment required is the same. Consequently, if we divide the process into a number of single-stage Hohmann orbital transfers between circular orbits, and if the velocity increment $\delta V_i'$ at each stage and the velocity increment δV_i in the transfer from the orbit of radius $r_{(i-1)}$ to the orbit of radius r_i found from Eq. (B-2) satisfy the relation:

$$\delta V_i>\delta V_i' \tag{B-3}$$

then we have proven that the cumulative value V_T of the velocity increments required for orbital transfer by means of continuous infinitesimal thrust is the maximum of values found using finite increments. The velocity increment $\delta V_i'$ required for single-stage Hohmann orbital transfer from the circular orbit of radius $r_{(i-1)}$ to the circular orbit of radius r_i is:

$$\delta V_i'=\{(\mu r_i/ar_{i-1})^{1/2}-(\mu/r_{i-1})^{1/2}\}$$
$$+\{(\mu/r_i)^{1/2}-(\mu r_{i-1}/ar_i)^{1/2}\} \tag{B-4}$$

where a is the semi-major axis of the intermediate orbit. Consequently, if we let e be the eccentricity and, $p= h^2/\mu=a(1-e^2)$, then we have:

$$\delta V_i=(h/p)\{(1+e)^{1/2}-(1-e)^{1/2}\} \quad \text{(B-5)}$$

$$\delta V_i'=(h/p)\{(2e+(1-e)^{1/2}-(1+e)^{1/2}\} \quad \text{(B-6)}$$

so that:

$$\delta V_i-\delta V_i'=2(h/p)\{(1+e)^{1/2}-e-(1-e)^{1/2}\} \quad \text{(B-7)}$$

Focusing attention on the terms enclosed in braces in Eq. (B-7), since:

$$\{(1+e)^{1/2}-e\}^2-(1-e)=e\{(1+e)^{1/2}-1\}^2 \quad \text{(B-8)}$$

the difference in Eq. (B-7) is always positive for e>0, proving that Eq. (B-3) is satisfied at every stage.

From the above discussion, as the number of stages of Hohmann orbital transfer is increased, the cumulative value of the required velocity increments increases, and asymptotically approaches the cumulative velocity increment V_T in the case of orbital transfer by continuous infinitesimal thrusting.

Further, if we let γ be the ratio of $\delta V_i'$ to δV_i, then from Eq. (B-5) and (B-6) we obtain the following equation:

$$\gamma =(1+e)^{1/2}+(1-e)^{1/2}-1 \quad \text{(B-9)}$$

Consequently, the ratio of the velocity increment V and V_t required for the Hohmann orbital transfer and the orbital transfer through continuous infinitesimal thrusting is determined. For reference, if we take r_s=7,378km and r_f=150,000km the eccentrity becomes 0.906 and we obtain γ=0.687. Consequently, the velocity increment required for the Hohmann orbital transfer is 69% of that required for orbital transfer through continuous infinitesimal thrusting.

<<Appendix C: The Error Sensitivity Coefficient Matrix Between Point P and Point Q>>

Letting δr_P and δr_Q be the position error vectors, and δv_P and δv_Q the velocity error vectors, at the P point and the Q point in the E-M coordinate frame, we introduce the vectors:

$$\delta z_P=\delta v_P/w \tag{C-1}$$

$$\delta z_Q=\delta v_Q/w \tag{C-2}$$

which are the velocity errors divided by the orbital angular velocity. Then, if we create the 6-dimensional vectors:

$$\delta x_P=[\delta r_P{}^T \delta z_P{}^T]^T \tag{C-3}$$

$$\delta x_Q=[\delta r_Q{}^T \delta z_Q{}^T]^T \tag{C-4}$$

and define the error sensitivity coefficient matrix K as:

$$\delta x_Q=K\delta x_P \tag{C-5}$$

then the elements of K are found by numerical calculation as those that satisfy the requirement that the δx_Q are produced from the δx_P.

For reference, we give the error sensitivity coefficient matrix between point P (10 days previous) and point Q for the polar entry orbit discussed in the text (Q point radius 45,000km, Q angle 0 degrees, Q point velocity 350m/s):

$$K=\begin{pmatrix} 2.23 & -2.71 & 0.82 & -1.43 & 5.94 & 1.18 \\ -1.82 & 0.71 & 0.20 & 1.02 & 1.59 & -0.02 \\ -1.66 & 1.13 & -0.77 & -0.93 & -2.13 & -0.59 \\ 10.0 & -5.26 & 1.50 & -5.33 & 10.0 & 1.00 \\ 16.7 & -2.63 & -3.38 & 9.33 & 5.00 & -1.70 \\ -2.07 & 5.64 & -3.01 & -2.00 & -12.8 & -4.70 \end{pmatrix} \tag{C-6}$$

where w=2.66x10^{-6}rad/s. Here linearity holds approximately between the limits of $\pm$ 1,000km for δr_P and $\pm$ 3m/s for δv_P; the values given in the above matrix are averages of the bipolar error sensitivity coefficients. In particular, the errors in the radial direction are strongly nonlinear and some bias occurs, but the width in the errors on either side is approximately linear.

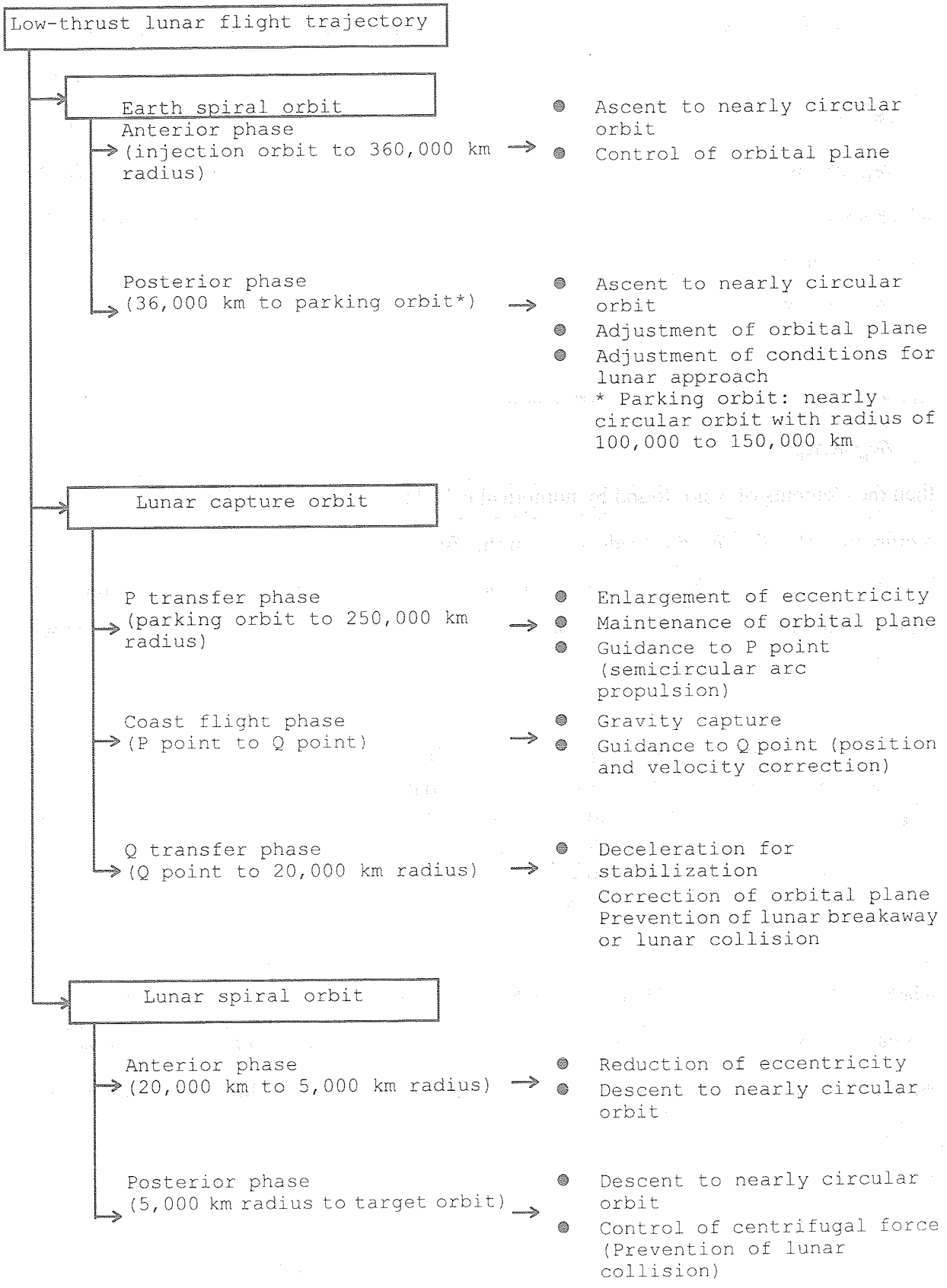

Figure 1 Configuration and control of low-thrust lunar flight trajectory

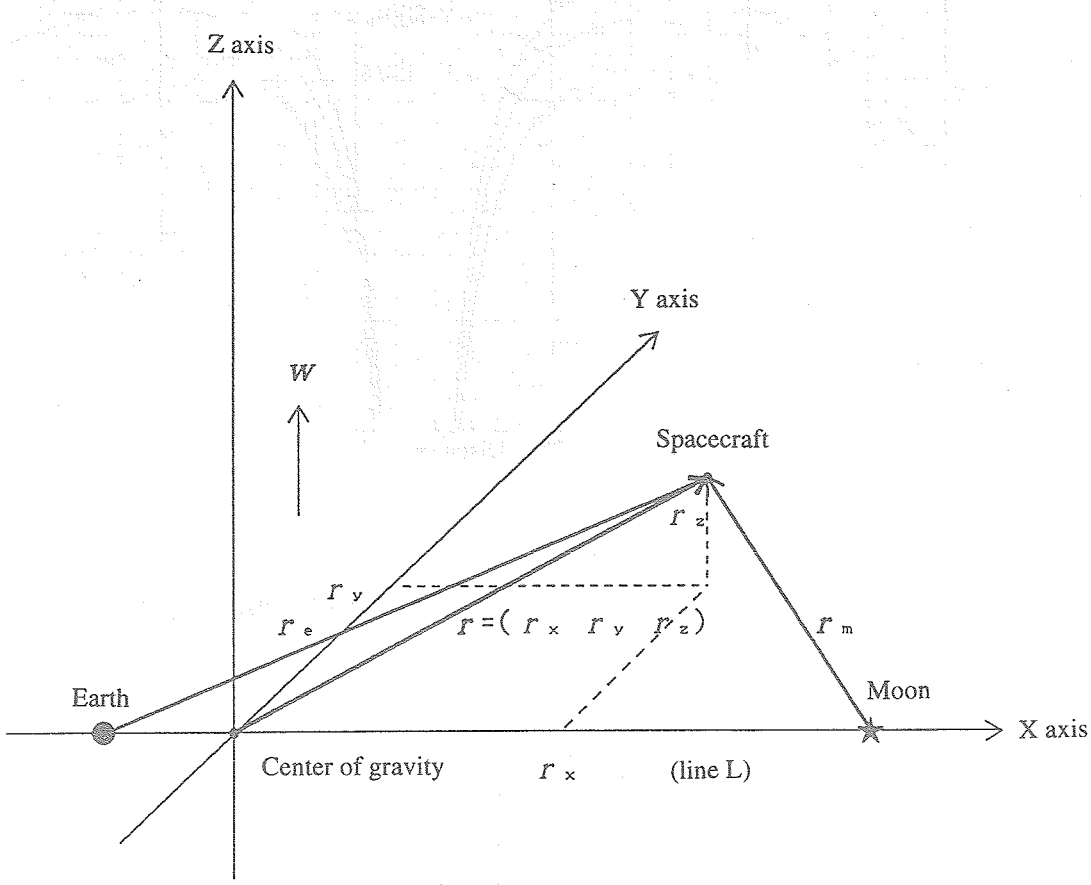

Figure 2 Earth-Moon fixed coordinate system (E-M coordinate system)

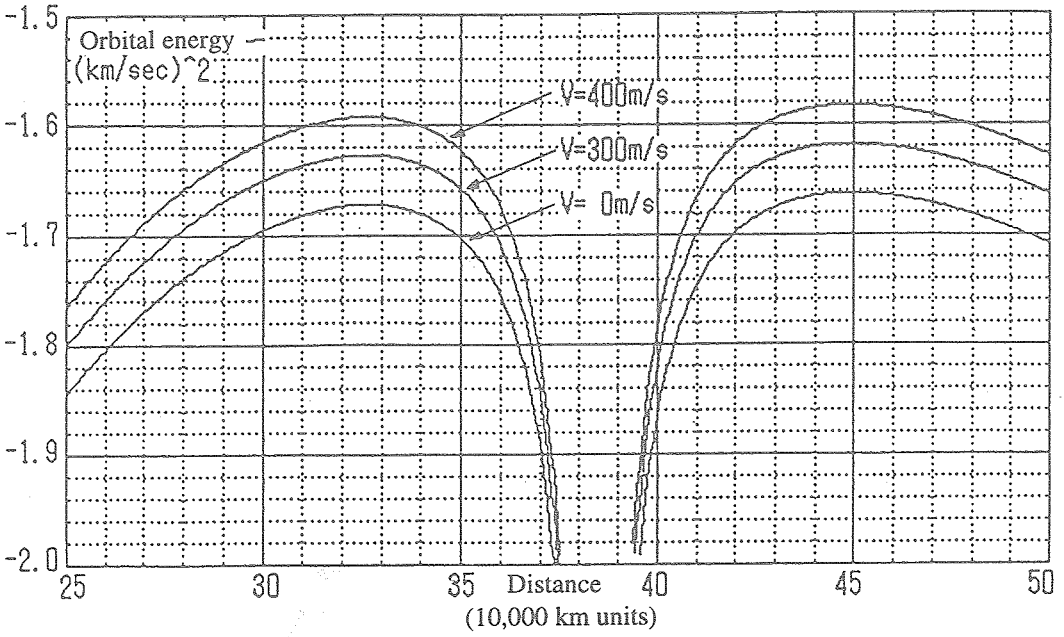

Figure 3 Orbital energy along line L connecting Earth and Moon

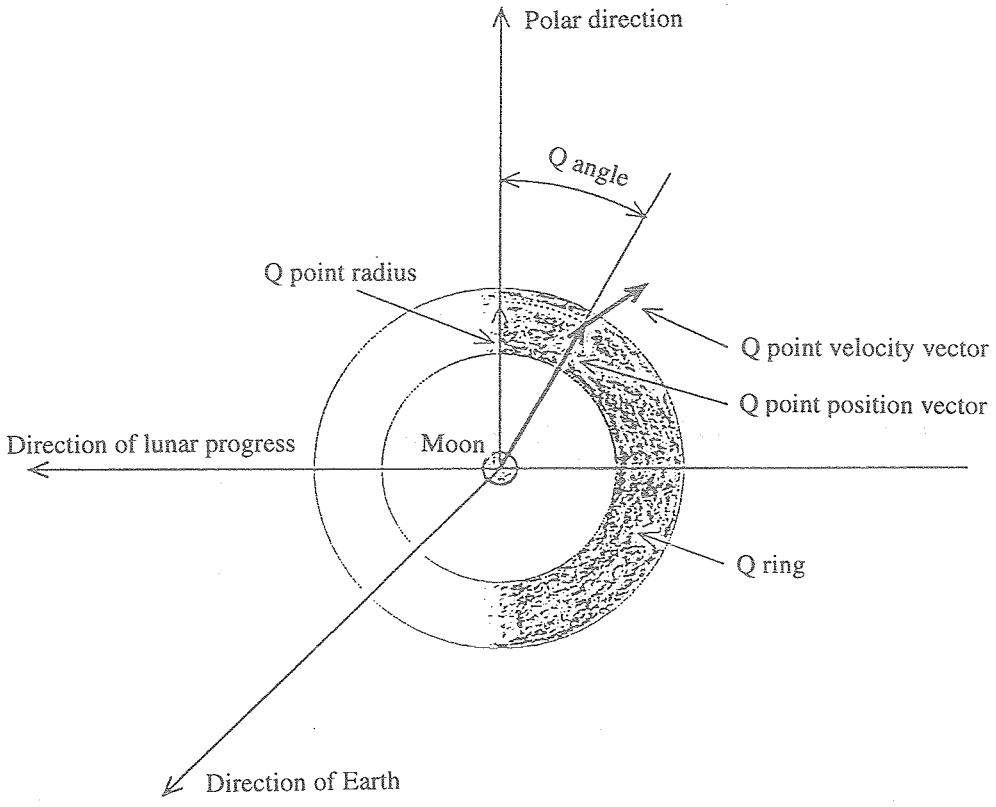

Figure 4 Conceptual diagram of Q point existence region

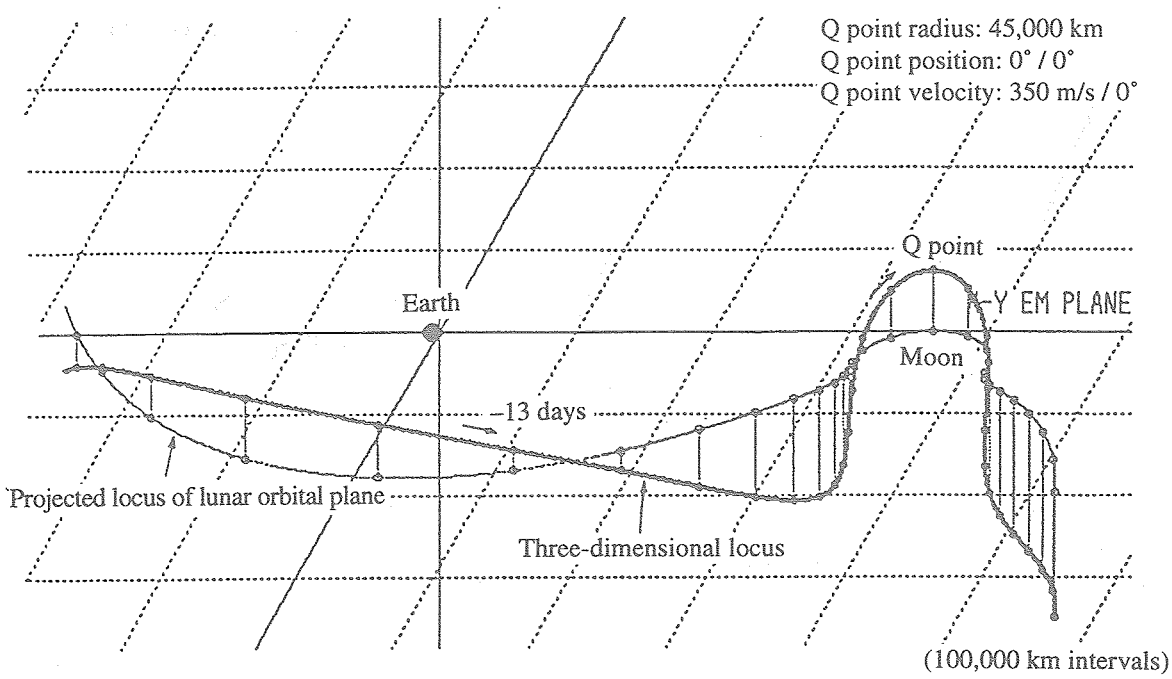

Figure 5 Example of flight trajectory for polar approach
(E-M coordinate system, Q angle = 0°)

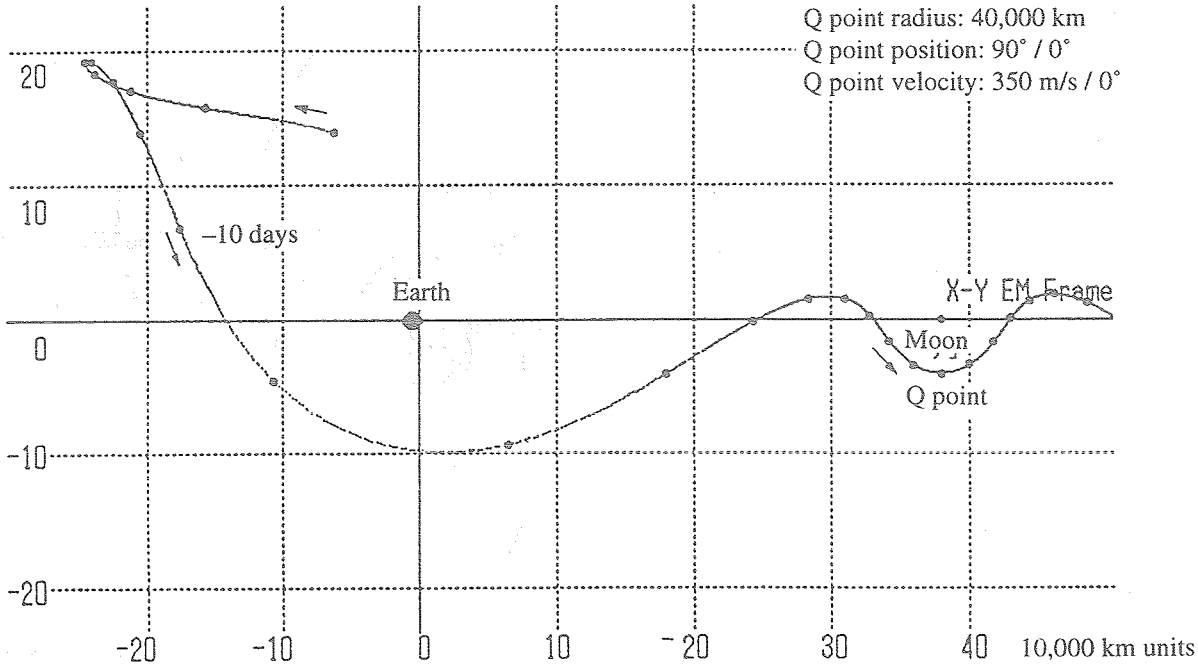

Figure 6 Example #1 of flight trajectory for equatorial approach
(E-M coordinate system, Q angle = 90°)

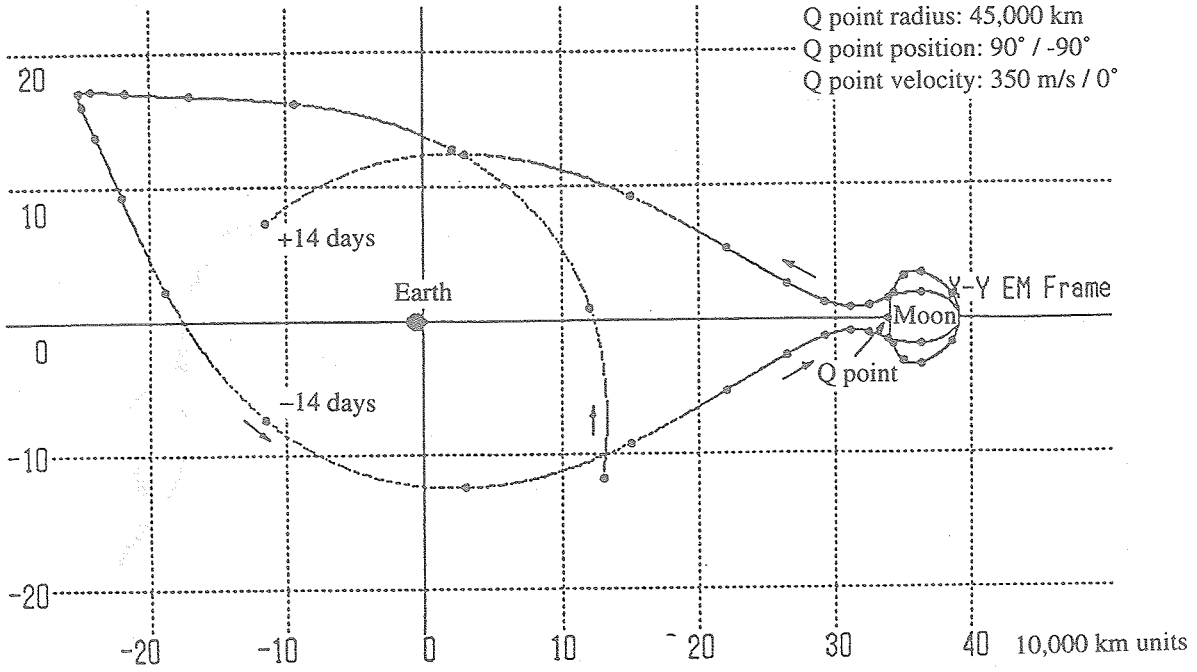

Figure 7 Example #2 of flight trajectory for equatorial approach
(E-M coordinate system, Q point on line L)

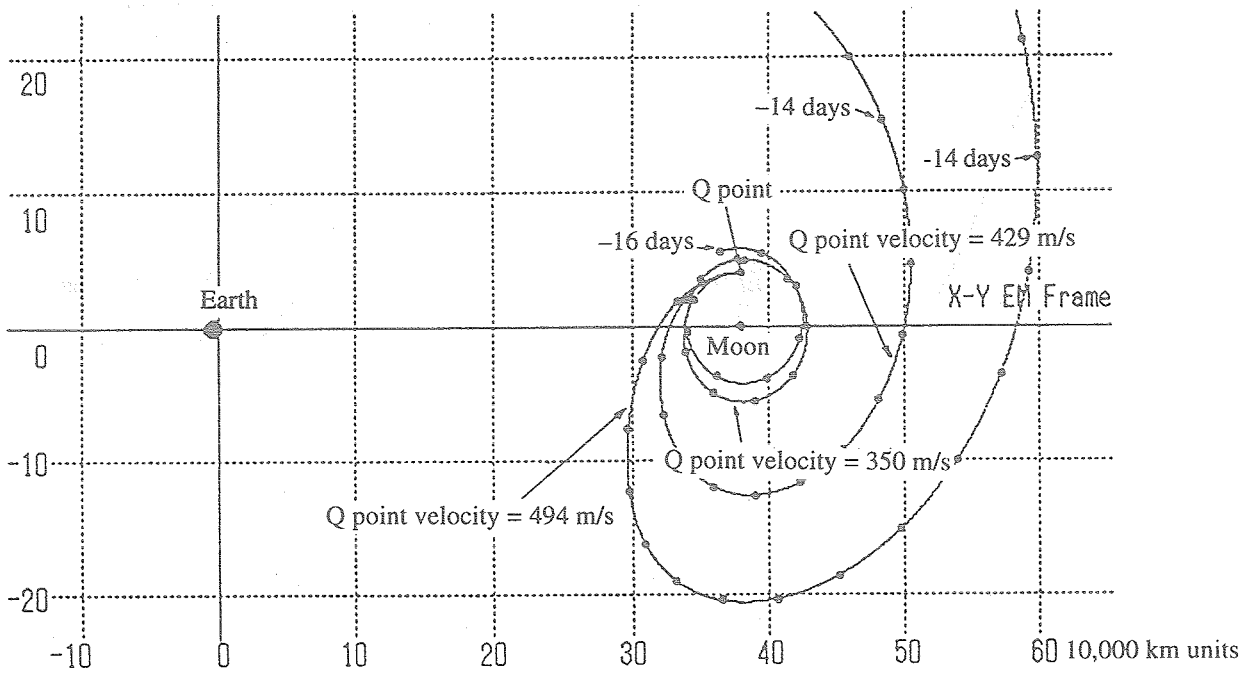

Figure 8 Example #3 of flight trajectory for equatorial approach
(E-M coordinate system, Q angle = –90°)

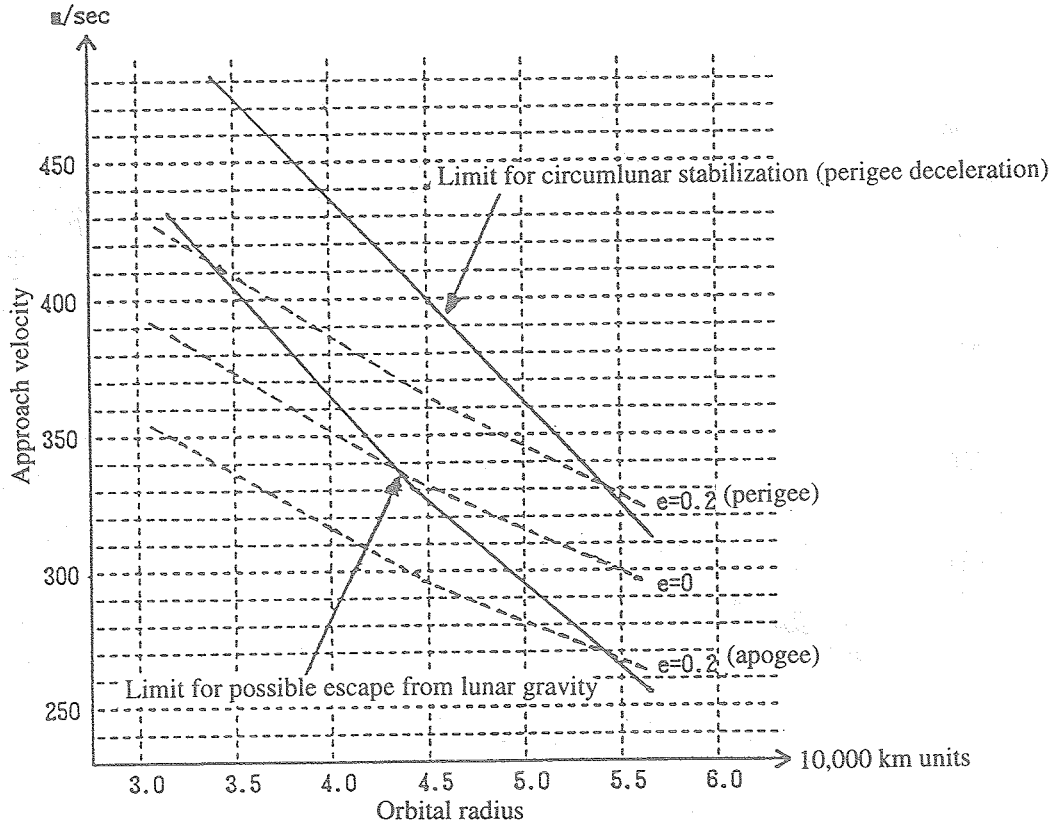

Figure 9 Conditions for establishment of Q point for polar approach trajectory (broken lines = fixed eccentricity curves)

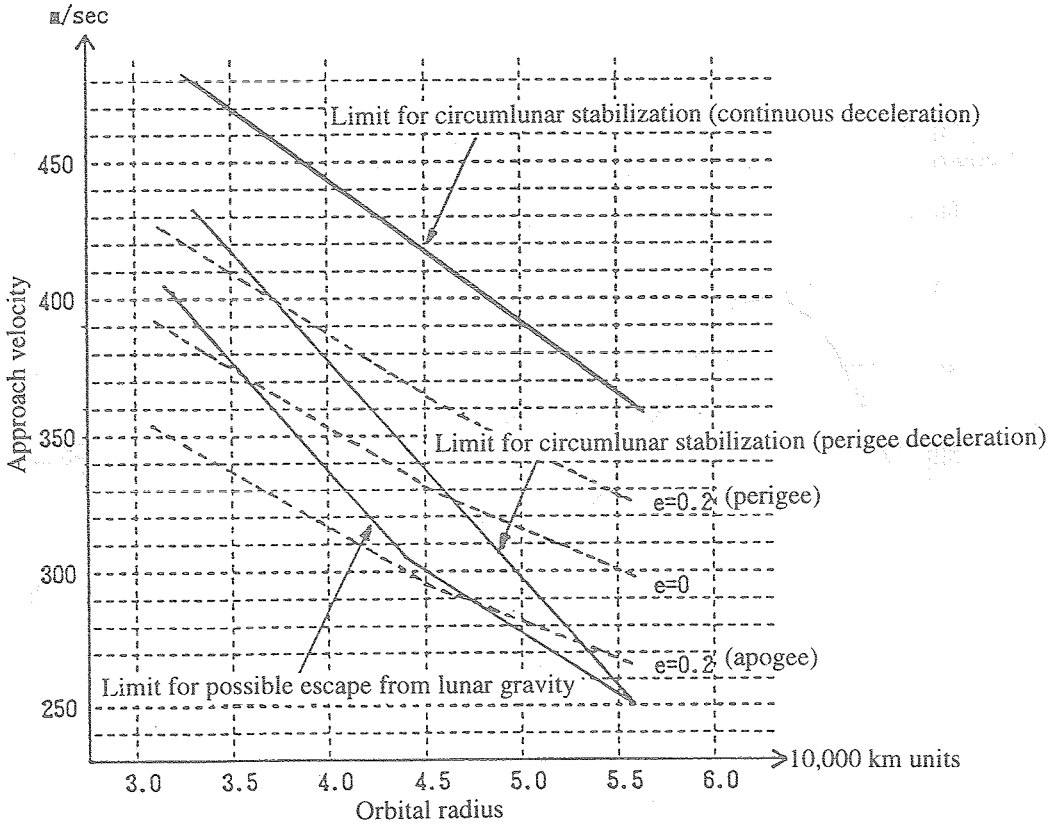

Figure 10 Conditions for establishment of Q point for equatorial approach trajectory (broken lines = fixed eccentricity curves)

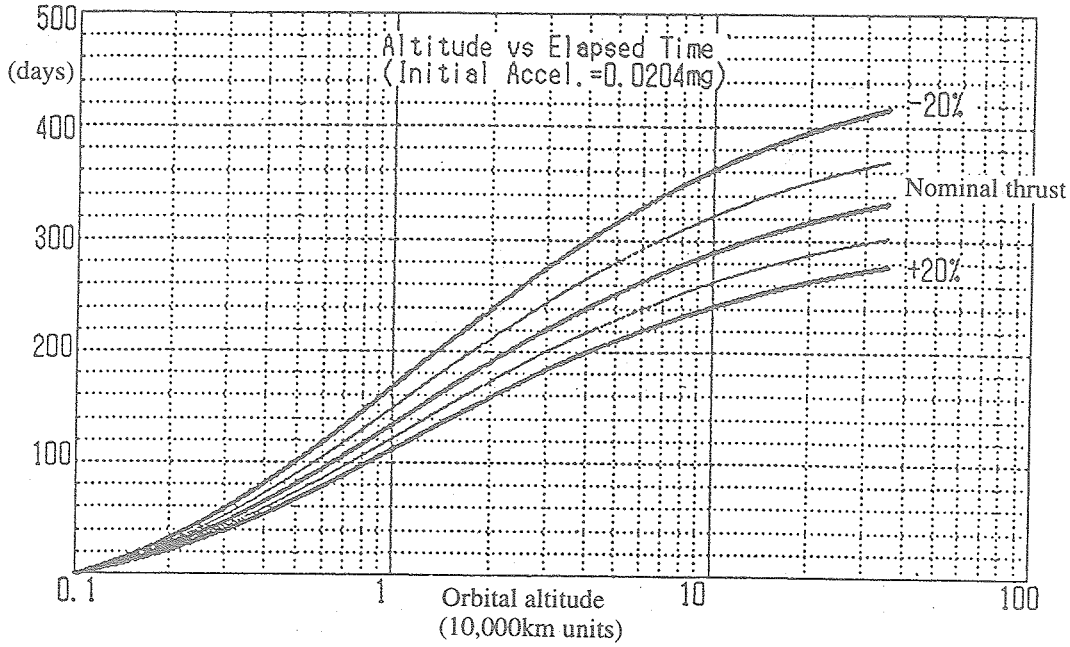

Figure 11 Relationship between orbital altitude and flight time
(3500 seconds thrust, 0.02mg initial acceleration)

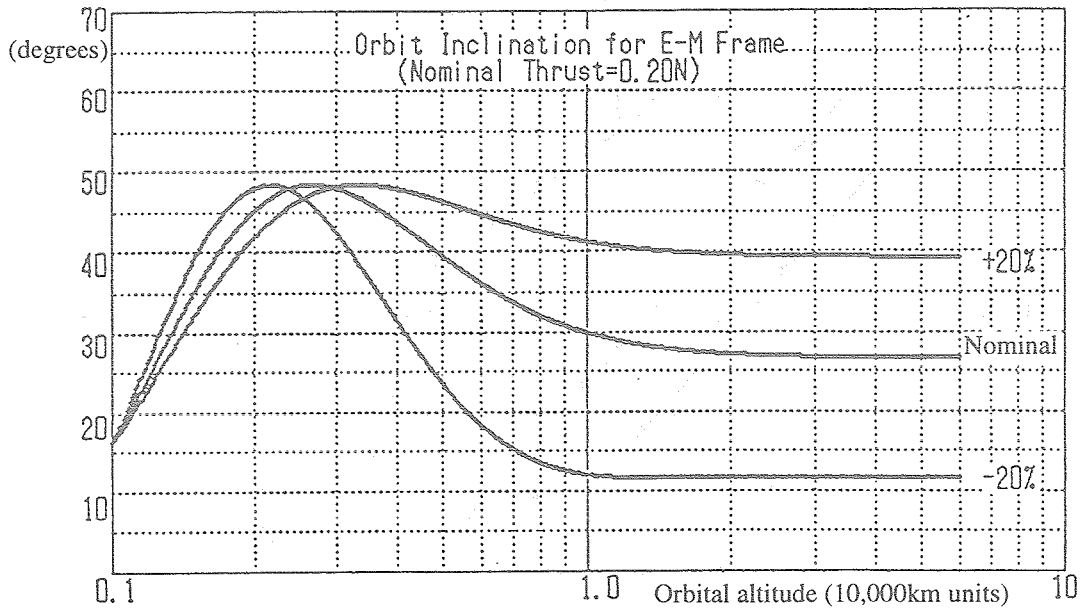

Figure 12 Relationship between orbital altitude and angle of inclination of orbital plane ($\Omega 0 = 330^\circ$)

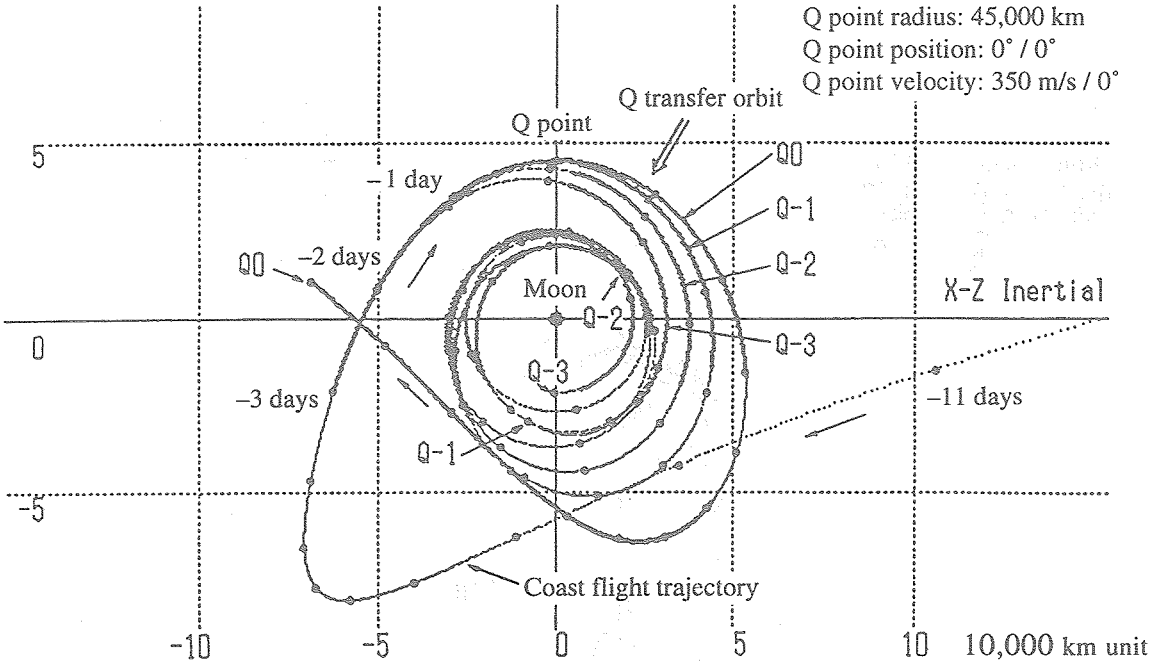

Figure 13 Relationship between date of initial deceleration and Q transfer orbit (showing trajectories for initial deceleration on three days before Q transfer, as well as on date of transfer)

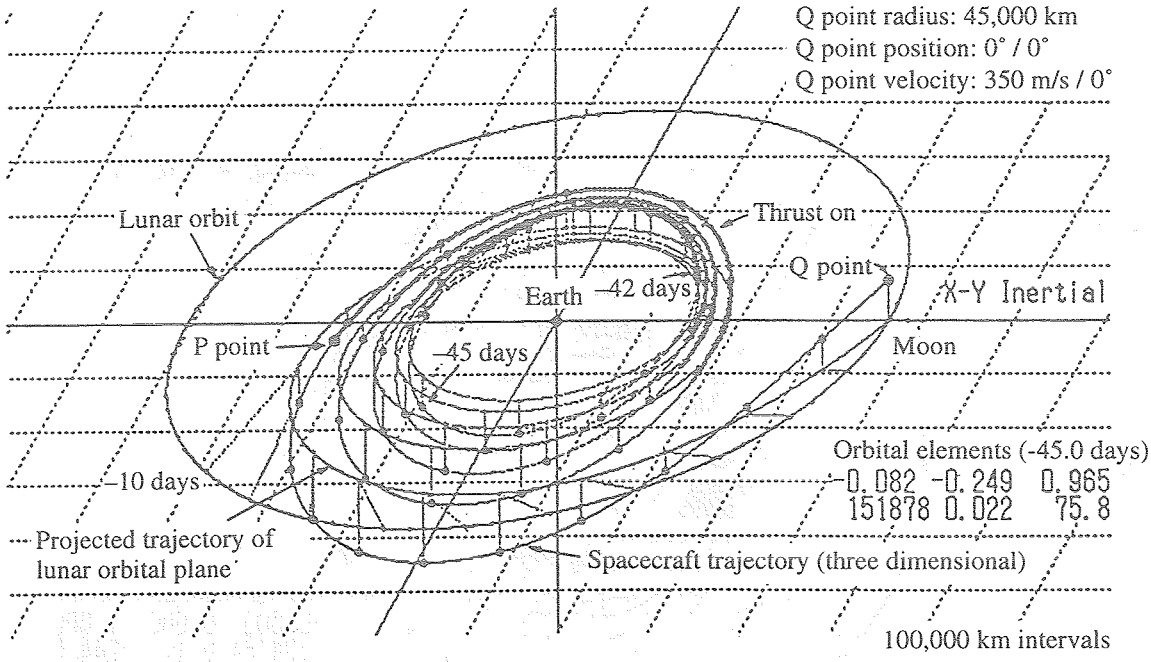

Figure 14 P point transfer orbit and coast flight trajectory for polar approach (shown in 3 dimensions, from –45 days to date of Q point transfer)

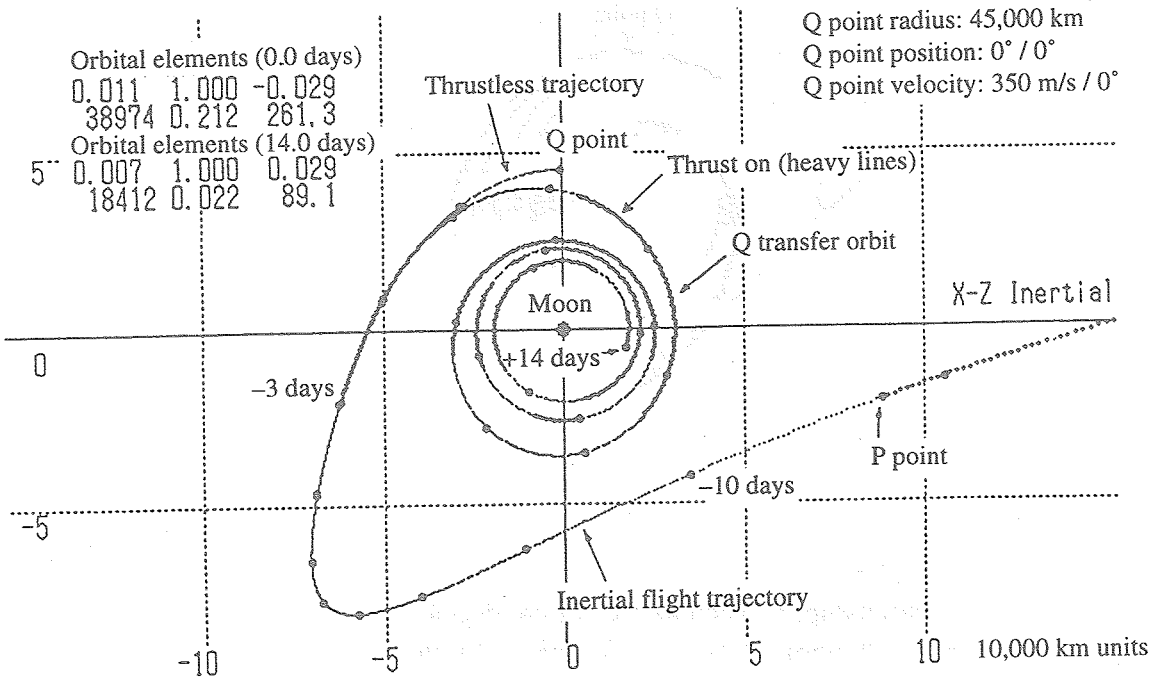

Figure 15 Stabilization of Q transfer orbit for orbital approach
(commencement of deceleration: -3 days)

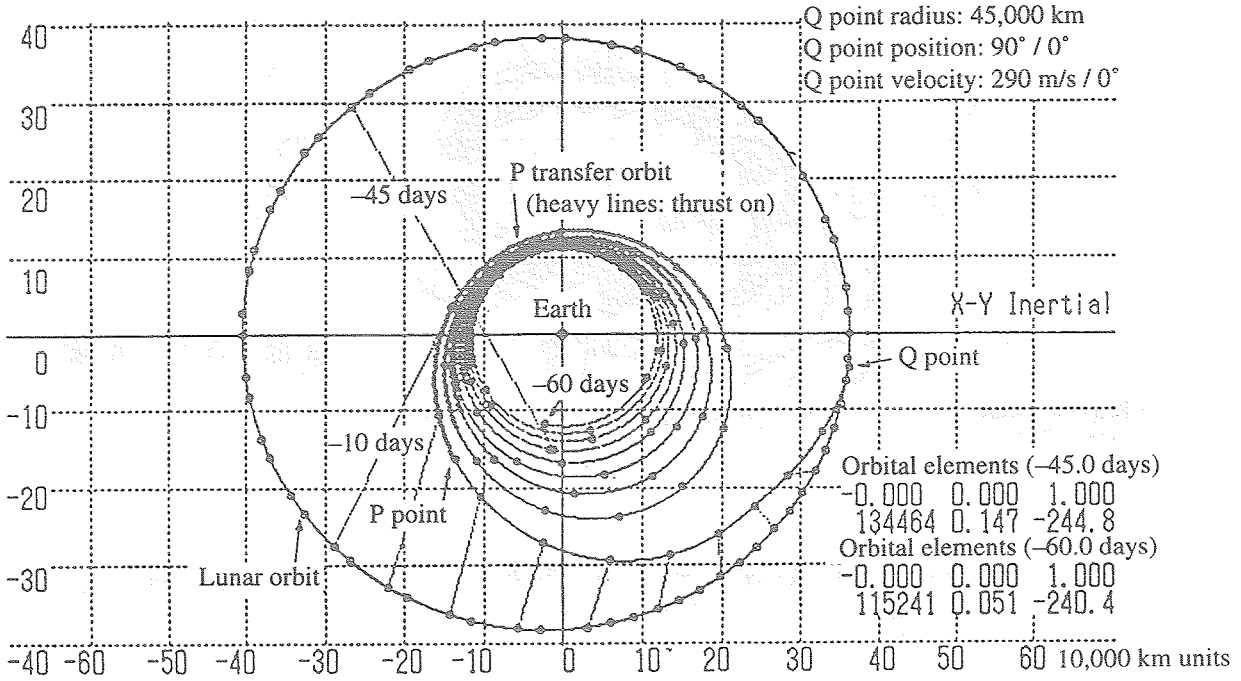

Figure 16 P point transfer orbit and coast flight orbit for equatorial approach
(from -60 days to Q point; Q angle: 90°

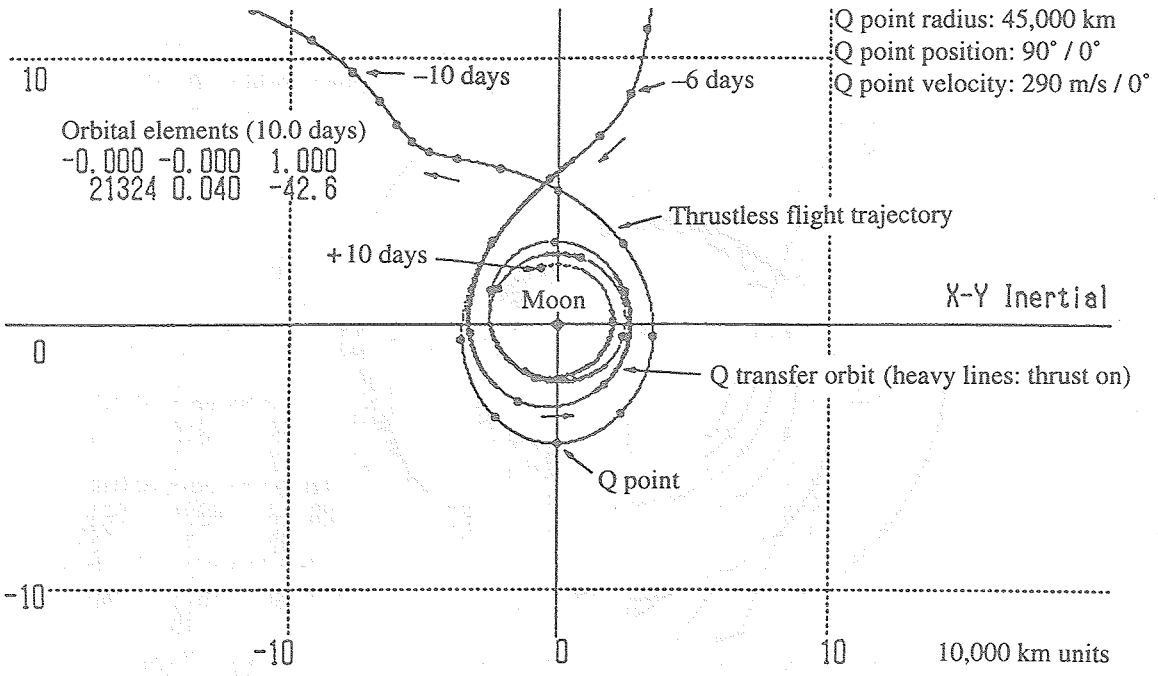

Figure 17 Stabilization of Q transfer orbit for equatorial approach
(commencement of deceleration: -4 days)

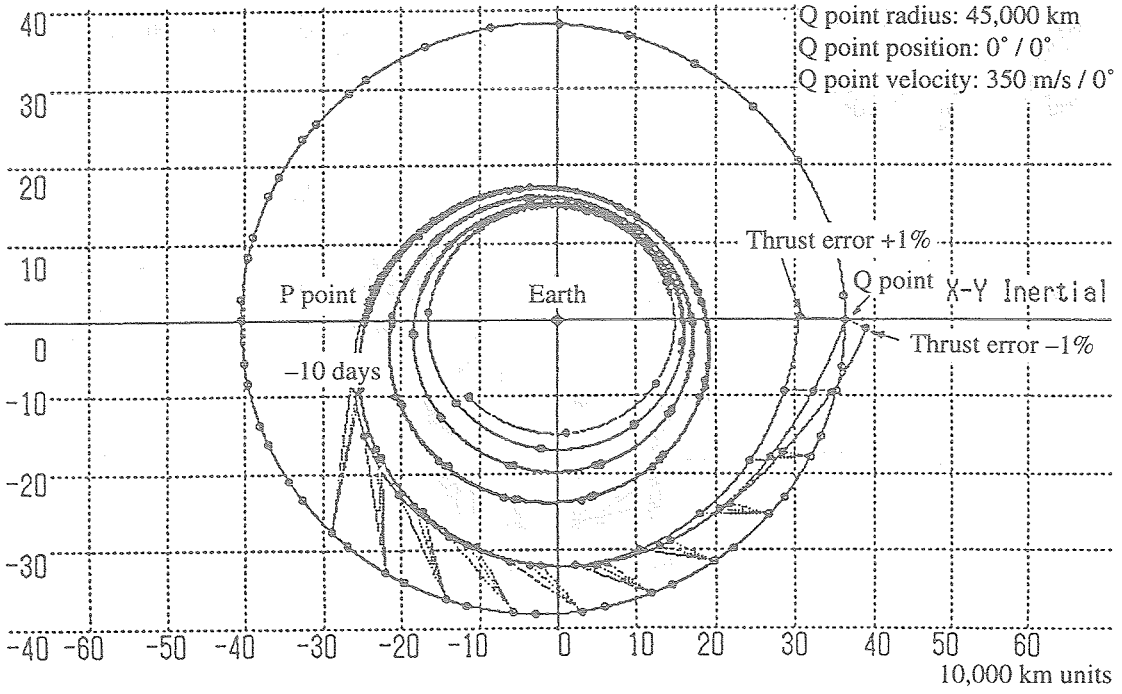

Figure 18 Coast flight trajectory error due to thrust error of P transfer phase (±1%)

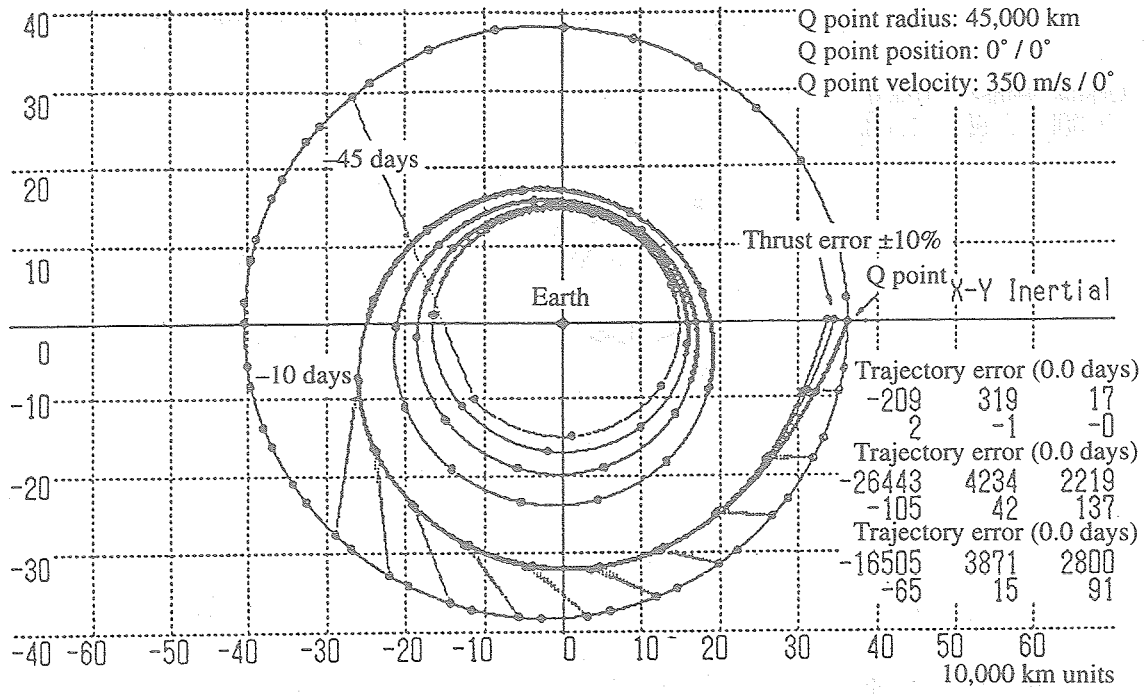

Figure 19 Effectiveness of thrust control method for counteraction of thrust error (±10%)

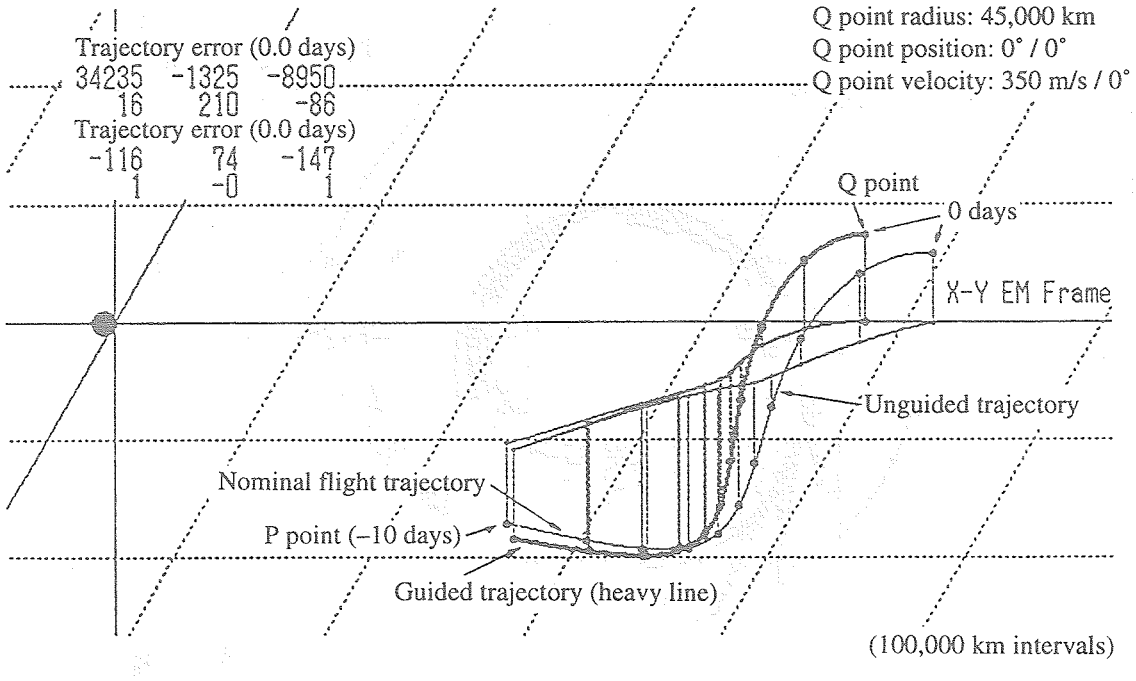

Figure 20 Influence of P point error on Q point, and effectiveness of perturbational guidance

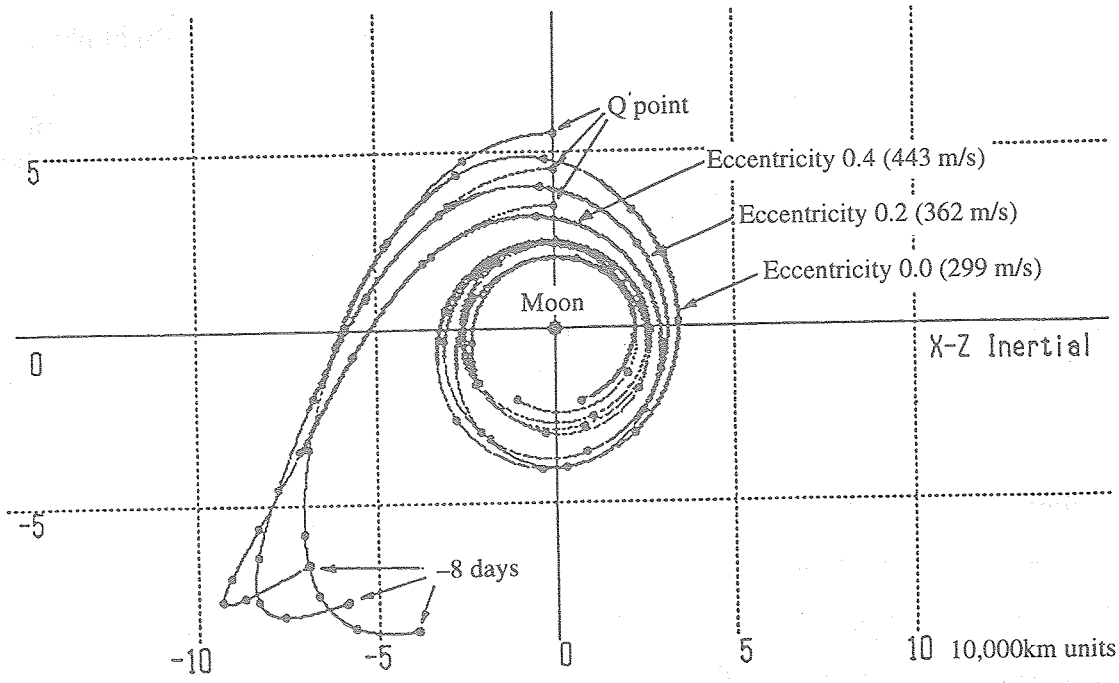

Figure 21 Relationship of Q point radius and velocity to Q transfer orbit

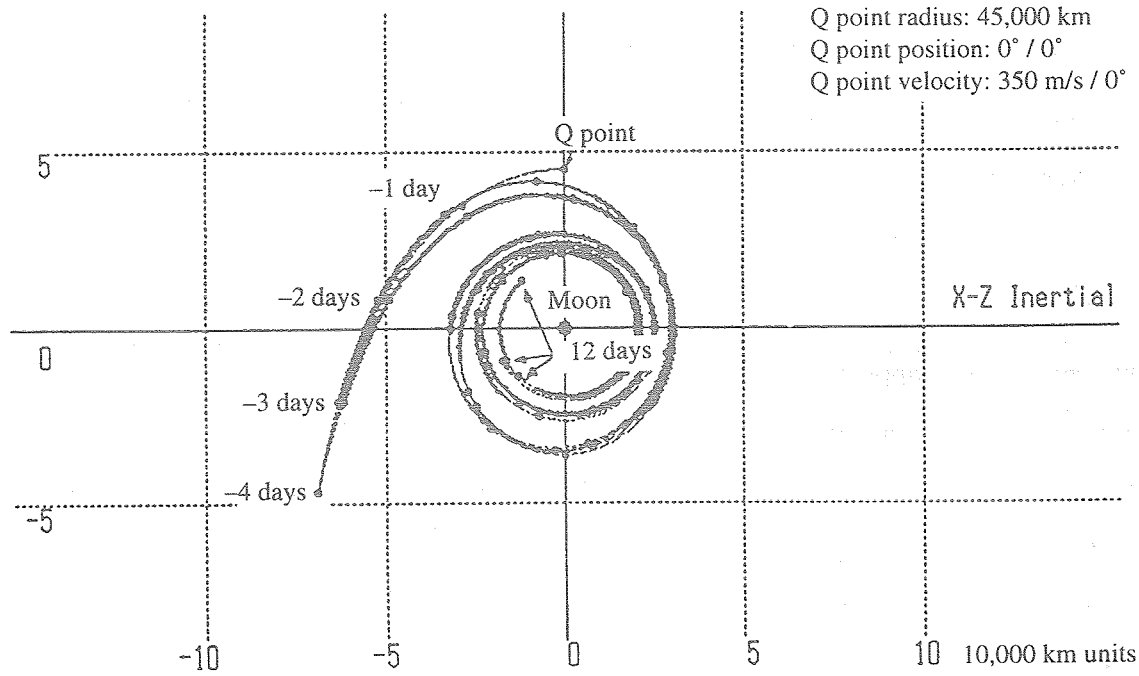

Figure 22 Relationship between Q point approach velocity error (=10 m/s) and Q transfer orbit

Table 1 Orbit control, required time, and propellant consumption for each flight phase

Orbit control for flight phases	Required time (in days)	Propellant consumed (%)
● Earth spiral orbit (approx. 10 months)		
◦ Earth spiral, anterior phase	220.6	11.1
◦ Ascent to nearly circular orbit (initial altitude: 10,000 km)		
◦ Adjustment of orbital plane angle of inclination(control of increase of orbital radius)		
◦ Earth spiral, posterior phase	84.3	4.2
◦ Maintenance of eccentricity and orbital plane (at no greater than 0.05 and 0.3[deg], respectively)		
◦ Adjustment of Q point intersection time		
● Lunar capture trajectory (approx. 2 months)		
◦ P transfer phase	31.7	0.8
◦ Enlargement of eccentricity (0.3 to 0.4)		
◦ P point guidance (thrust on/off sequence control)		
◦ Average thrust adjustment		
◦ Coast flight phase	10.6	1.3
◦ Trajectory correction (perturbational guidance)		
◦ Q transfer phase	15.7	0.4
◦ Deceleration control		
◦ Reduction of eccentricity (to about 0.2)		
● Lunar spiral orbit (approx. 2 months)		
◦ Lunar spiral, anterior phase	23.4	1.2
◦ Reduction of eccentricity (to no greater than 0.05)		
◦ Descent to nearly circular orbit		
◦ Lunar spiral, posterior phase	29.9	1.5
◦ Maintenance of eccentricity (at no greater than 0.02)		
◦ Descent to nearly circular orbit		
Total	416.2	20.5

NASDA Technical Memorandum (NASDA-TMR-950006T)
Date of Issue : October 15, 1996
Edited and Published by :
National Space Development Agency of Japan
2-4-1, Hamamatsu-cho, Minato-ku,
Tokyo, 105-60 Japan

Inquiries and suggestions on the Report
should be addressed to :
Technical Information Division
External relations Department
2-4-1, Hamamatsu-cho, Minato-ku,
Tokyo, 105-60 Japan
FAX : +81-3-5402-6516
* This report is an English version of NASDA-TMR-950006

NASDA

NATIONAL SPACE DEVELOPMENT AGENCY OF JAPAN